

ALMA MATER STUDIORUM – UNIVERSITÀ DI BOLOGNA

DOTTORATO DI RICERCA IN

INGEGNERIA ELETTRONICA, TELECOMUNICAZIONI E
TECNOLOGIE DELL'INFORMAZIONE

CICLO 32°

Settore Concorsuale: 09/E3 - ELETTRONICA

Settore Scientifico Disciplinare: ING-INF/01 - ELETTRONICA

Wireless Sensor Networks for Advanced Industrial and Biomedical Applications

Presentata da:

Massimo Ballerini

Coordinatore Dottorato:

Prof. Alessandra Costanzo

Supervisori:

Prof. Luca Benini

Ing. Guido Comai

Esame Finale Anno 2020

Abstract

In the modern industry, data processing systems must be able to receive, aggregate, and process information from different sources to achieve complex tasks of production control and coordination. Examples are the real-time monitoring of the quality and quantity of products, biometric data acquisition in the rehabilitation procedures. Energy efficiency in the data communication system is essential in wireless networks. Reduce power consumption in the data exchange can prolong the operating life of battery-powered devices and save energy on a global scale. In this direction, a fundamental step is to accurately model the energy consumption for data communication over a wireless link for the system of interest. The first part concerns the application scenario of the Body Sensor Network for motion reconstruction applications. Wireless systems that use wearable sensors have developed rapidly in recent years, and the requirements in terms of throughput and timing accuracy are challenging. This thesis presents a new general-purpose Inertial Measure Unit that exploits a dual-core architecture. A core offers processing capability, and the other one is a radio interface IEEE 802.15.4. I propose the whole system and a protocol to maximize the throughput, reduce the packet loss, and improve the robustness of wireless sensor nodes communication. In the second part of the thesis, I move the attention to the Low Power Wide Area Network in the IoT scenario. Today, the most promising long-range communication technologies are LoRaWAN and Narrow Band IoT (NB-IoT), which are driving a vast IoT ecosystem. A dedicated chapter evaluates the performance of LoRaWAN and NB-IoT with accurate in-field measurements using the same monitoring application for a comparison in terms of energy efficiency, lifetime, quality of service (QoS), and coverage. Finally, the last part provides configuration guidelines for future industrial applications with harsh requirements of long-range and low power wireless connectivity.

Acknowledgements

The research contribution presented in this Industrial Ph.D. thesis has been funded by a research grant of MediCon Ingegneria.

Contents

1	Introduction	7
1.1	Objectives	8
1.2	Contributions	9
2	MAC Layer Protocols for WSN & IoT	13
2.1	Short Range	14
2.1.1	Bluetooth IEEE 802.15.1	14
2.1.2	Bluetooth Low Energie	15
2.1.3	IEEE 802.15.4	16
2.2	Long Range	17
2.2.1	LoRa and LoRaWAN	17
2.2.2	Sigfox	19
2.2.3	NB IoT	21
2.3	Conclusion	23
3	Wireless Inertial Sensors Network	25
3.1	Body Sensor Networks	25
3.1.1	BSNs Applications and Open Issues	25
3.1.2	Goals, Challenges and Insights	26
3.2	System Architecture	27
3.3	Hardware Implementation	28
3.3.1	Wireless Inertial Sensor	29
3.3.2	Gateway	31
3.4	Antennas Analysis	32
3.4.1	Antenna Selection	33
3.4.2	Link Budget	34
3.5	Wireless Communication Protocol	35
3.5.1	Setup Phase	37
3.5.2	Working Phase	38
3.6	Firmware Implementation	39
3.6.1	SMAC	39
3.7	Experimental Results	41
3.7.1	Throughput and scalability	41
3.7.2	Packet Loss	43
3.7.3	Power Consumption	44

4	NB-IoT vs. LoRaWAN	45
4.1	Related Works	45
4.2	Experimental Setup	47
4.2.1	The SHM sensor node	47
4.2.2	LoRaWAN End-Device Setup	48
4.2.3	NB-IoT End-Device Setup	49
4.3	Experimental Results	49
4.3.1	LoRaWAN End-Device Analysis	49
4.3.2	NB-IoT End-Device Analysis	50
4.3.3	Battery life and comparisons	53
5	Long-Range Deployments Guidelines	56
5.1	Quality of Service and Coverage	56
5.2	Cost and Time To Market	56
5.3	Security	57
6	Conclusion	58
	Bibliography	69

List of Figures

1.1	WSN in IoT system. An extensive collection of wireless sensors can be used to send data through a router to the internet. In these cases, WSN is an integrated part of the IoT system.	9
2.1	Bluetooth IEEE 802.15.1 Stack	14
2.2	BLE Stack	16
2.3	IEEE 802.15.4 Stack	17
2.4	LoRaWAN Topology.	18
2.5	Sigfox protocol stack.	20
2.6	Operation modes for NB-IoT.	21
2.7	Extended Discontinuous Reception: the periodicity value of the reception windows can reach 10.24 s in Connected and 2.91 hours in Idle state, respectively. Power Saving Mode: device remains registered with the network, and it is not necessary to re-attach or re-establish the connection. The maximum duration of the PSM mode is 310 hours.	22
3.1	Overview NETWIS system: several WIS devices communicate the data acquired to the high-level application via the GW, a central node in a star network.	27
3.2	NXP Kinetis K22 Microcontroller and NXP Kinetis KW41Z Microcontroller family features.	29
3.3	Blocks diagram WIS unit: the dual-core platform incorporates a digital magnetometer, a gyroscope, and two analog accelerometers.	30
3.4	WIS unit: the dimensions are 40 mm x 30 mm, the weight is 20 g.	31
3.5	Blocks diagram GW unit.	31
3.6	GW unit: the dimensions are 80 mm x 20 mm.	32
3.7	Omnidirectional antenna diagram except for two minima at theta near + 90 ° and -90 ° degrees. It is necessary to avoid the antennas orientation that involves the direction of the connection in correspondence with these minima.	33
3.8	Communication Round.	36
3.9	T slot.	36
3.10	Bootstrap: the nodes must be connected to the GW on an unknown channel a priori.	37
3.11	Scheduling in NETWIS with five nodes: the T_{round} is the reciprocal of the WIS sampling rate set by the GW. The slot time T_{slot} can be set up to 5 ms. For transmission of a 19 bytes message, 1.5 ms is sufficient in practice.	38

3.12	Dual-core operations: unit K_i is woken synchronously when the broadcast message is received on the KW_i . In this way, all the network units remain aligned.	39
3.13	SMAC Architecture	40
3.14	Throughput for several pairs N , $f_{refresh}$ with slot equivalent 1.5 ms and Simplex mode configuration.	41
3.15	The maximum operating frequency according to the operating mode: the payload is 19 B for Simplex, 25 B for Medium, and 49 B for Raw.	43
4.1	Low power wireless crack-meter.	47
4.2	NB-IoT characterization with median, 25th, and 75th percentiles. Good (G) in green with an average RSSI of -80dBm, Medium (M) in orange with an average RSSI of -110dBm and, Red (R) with an average RSSI of -130 dBm.	51
4.3	Differences between single and multiple packet transmissions in a single connection.	53
4.4	Expected battery lifetime and EPB with LoRaWAN and NB-IoT. End-device coverage is divided into: DR0/Bad with an average RSSI of -130 dBm, DR2/Medium with an average RSSI of -110dBm and, DR5/Good with an average RSSI of -80dBm.	55

List of Tables

3.1	CoreMark and Dhrystone per MHz performance benchmarks for the ARM Cortex-M series (Courtesy of ARM).	30
3.2	Link Budget	34
3.3	IEEE 802.15.4 - Tx Power set = -15 dBm	34
3.4	IEEE 802.15.4 - Tx Power set = -9 dBm	34
3.5	IEEE 802.15.4 - Tx Power set = -3 dBm	35
3.6	IEEE 802.15.4 - Tx Power set = 0 dBm	35
3.7	Throughput T_{Slot} 1.5 ms	42
3.8	Throughput T_{Slot} 1.4 ms	42
3.9	Packet Loss	44
3.10	Power Consumption	44
4.1	LoRaWAN EPB & EPP	49
4.2	NB-IoT Energy Characterization	51
4.3	NB-IoT EPB	52

Chapter 1

Introduction

Internet of things (IoT) is a neologism related to the Internet extension to the world of objects and places. The term "IoT" was initially introduced to refer to uniquely identifiable interoperable connected objects with Radio-Frequency Identification (RFID) technology [1]. Recently, researchers have described IoT in various forms:

- *"The Internet of Things (IoT), also called the Internet of Everything or the Industrial Internet, is a new technology paradigm envisioned as a global network of machines and devices capable of interacting with each other. The IoT is recognized as one of the most important areas of future technology and is gaining vast attention from a wide range of industries." ([2])*
- *"The Internet of Things is a paradigm where everyday objects can be equipped with identifying, sensing, networking and processing capabilities that will allow them to communicate with one another and with other devices and services over the Internet to accomplish some objective." ([3])*
- *"The Internet of Things is a vision, which is currently under progress. The idea to connect everything and anything and anytime is appealing. The dynamic nature of IoT and the scale on which it will be functional is hard to imagine and thus there will be huge responsibility to overcome the challenges." ([4])*
- *"The IoT is a broadband network that uses standard communication protocols while its convergence point is the Internet. The main concept of the IoT is the universal presence of objects that can be measured, inferred, understood and that can change the environment." ([5])*

The IoT technologies, considering the wide variety of uses and the diversity of functionalities required to satisfy more innovative applications, are advancing at a fast pace to meet this demand [6]. The IoT revolution arrives at its decisive moment, the one in which it will change the institutions and operating companies. Business Insider imagines this scenario Intelligence with the theme "The IoT Forecast Book 2018" [7]. As for corporate IoT, companies continue to invest dollars in connected devices and automation. By 2023, the total installed base of industrial robotic systems will reach 6 million worldwide, while the annual expenditure for the production

of IoT solutions will reach approximately 450 billion dollars. Services around the world are introducing IoT systems for developing smart cities. Annual investments in this sector are expected to reach nearly \$ 900 billion by 2023. The main areas of application of the IoT (both for end consumers and for companies) are represented by those contexts in which there are "things" that can generate new information such as: smart home, home automation, smart building, building automation, industrial monitoring, robotics, collaborative robotics, automotive, self driving car, smart health, healthcare, the biomedical world, smart city, smart mobility, new forms of digital payment through objects, smart agrifood, wearable for animals [8].

The IoT potentials in the industrial world are huge: an interconnected system makes it possible to speed up communication between different devices that perform entirely different tasks and therefore allow better interaction between them, thus optimizing the production process. Consider, for example, an assembly line where different parts from other chains must be assembled. The IoT makes it possible to easily pass all those pauses deriving from delays or unforeseen events that could create significant problems, making the equipment communicate directly with each other so that they can autonomously regulate their work cycle. Furthermore, in addition to being physically interconnected, all the machines are joined to integrated company systems, which manage the production, safety, and administrative aspects.

1.1 Objectives

The IoT development in society and everyday life draws at the same pace sensor networks. In addition to applications, where mobility is an intrinsic feature of the system, there are many other scenarios where wired connectivity is difficult to achieve due to logistics and cost problems.

Wireless Sensor Network (WSN) is one of the critical parts of the IoT system [2, 9]. A WSN is a wireless network consisting of spatially distributed autonomous devices using sensors to monitor physical or environmental conditions cooperatively. In a typical scenario, users can retrieve information of interest from a WSN by requesting queries from the base stations, which is the interface between users and the network(Figure 1.1).

The onboard sensors on the wireless node collect information about the environment and positioning data. The philosophy behind WSNs is that, while the capability of each sensor node is limited, the aggregate power of the entire network can perform the required mission. WSNs can be deployed on a global scale for environmental monitoring, over a battle-field for military surveillance, in factories for smart Industry, in buildings for infrastructure health monitoring, or on bodies for patient monitoring. Many examples of applications can be found in [6].

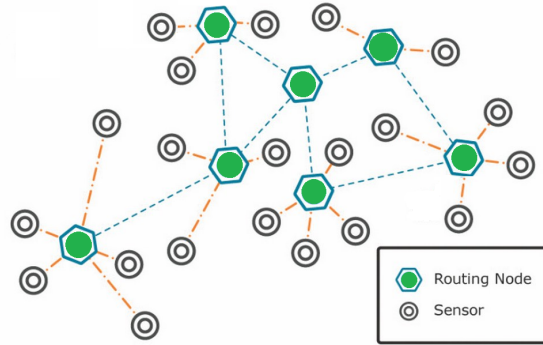


Figure 1.1: WSN in IoT system. An extensive collection of wireless sensors can be used to send data through a router to the internet. In these cases, WSN is an integrated part of the IoT system.

Primarily energy efficiency, scalability, reliability, and robustness parameters are examined when designing a WSN system. Therefore, considering the data expressed in the first part, it is natural that the research of the various technologies in the WSN world is an exciting theme in the industrial world. From this aspect comes the aim of this industrial Phd., which is to be able to master the different aspects that present themselves to a consulting company to decide which solution is best suited for the realization of business and an entrepreneurial idea in the most diversified fields.

1.2 Contributions

The Body Sensor Network (BSN) technology is one of the core technologies of IoT developments in the healthcare system, where a patient can be observed using a collection of wireless sensor nodes [10]. In the last decades, many BSNs have been realized, for instance, with commercial architectures such as Xsens and Shimmer [11, 12] or with customized solution [13, 14, 15, 16]. Even if the BSN sensors are exclusively connected with a specific wireless technology, therefore not belonging to the purely IoT world, they are usually connected to a particular node with an internet interface. This node usually has the master functions of the BSN star network. Thus, the overall system falls under the definition of an IoT object.

Motion capture (MoCap) is a way to record human movements digitally. The recorded motion capture data is mapped on a digital model in 3D software, so the people's moves are recorded. The primary purpose of this technology is to monitor people's movements for rehabilitation or sporting purposes [17, 14]. MoCap technology also is used in the entertainment industry for films and games to get more realistic human movements. Clinical rehabilitation is one of the driving sectors for the IoT world.

Wearable technology, which is in close contact with the user, is often used to monitor a user's performance. Wearable devices can be used to collect data on a

user's health, e.g., heart rate, steps walked, blood pressure. These functions are often together in a single unit, like an activity tracker or a smartwatch like the Apple Watch Series 2 or Samsung Galaxy Gear Sport. Devices like these are used for physical training and monitoring overall physical health. At the end of the session, the data collected by the sensors and processed by the software are sent to the cloud. The therapist can access it at any time to check the progress of the rehabilitation and, if necessary, to adjust the exercises. The quantitative detection of the parameters through the use of sensors also contributes to improving the objective measurement of treatment results and supports the creation of a rehabilitative cloud database. The database, in perspective, will be able to ensure an enormous predictive value, thus making it possible to treat other patients more efficiently and effectively thanks to the optimization of care.

This work presents a novel hardware-software architecture for a system motion capture in Chapter 3. In detail, the main activities and contributions of this thesis for this part are the following:

- development of inertial wireless sensors able to directly execute generic localization calculation algorithms based on data sampled by accelerometers, magnetometers, and gyroscopes.;
- Implementation of a protocol to optimizing throughput, synchronization, and scalability over BSNs.
- development of wearable network devices for motion capture application purposes;

The developed platform is employed for the analysis of new magnetometer calibration algorithms [18]. Experimental results show the benefits of the proposed solution in terms of throughput, scalability, power consumption, and percentage of packets lost.

Another important key factor in the IoT and WSN world is the industrial one. Industry 4.0 [19] is the term that describes a new generation of autonomous wireless devices, which pervasively connect machines and objects, creating a new domain called Industrial Internet of Things (IIoT) [20, 21]. More and more practical applications can be found today, whose types of communication architectures belong to these three macro-categories [22]:

- XMBB: Xtreme Mobile Broadband Communications
- UMTC: Ultra-reliable Machine-Type Communications
- MMTC: Massive Machine-Type Communications

The XMBB provides high data rates in the range of Gbps. For example, consider a crowded stadium where all users want to enjoy 3D streaming of the match on their smartphone. The UMTC deals with ultra-reliable and time-efficient devices. For example, think of the safety of a pedestrian concerning a vehicle. Another type of UMTC is reliable communication for manufacturing in factories. The MMTC

enables 5G services to lots of devices with energy efficiency [21]. For example, we can think of security monitoring, smart home, smart building, and smart environment.

In the MTC devices domain, Low-Power Wide-Area (LPWA) technologies are targeting these emerging applications and markets. Consequently, different technologies are needed, thereby introducing new challenges in terms of energy efficiency [23]. Among them, low power consumption and communication range are crucial for IIoT devices and are further exacerbated by battery lifetime requirements. Hence it is not surprising that in recent years, many approaches have been proposed to improve them [24, 25].

Following the rapid IoT market expansion, LPWAN became one of the faster-growing areas in IoT. LPWAN is the common term to identify the wireless technologies that enable wide-area communication at low cost and low power consumption. The LPWAN typical application scenario needs to transmit a few bytes for long ranges. Many LPWAN technologies are emerging in both licensed and unlicensed markets, such as LoRaWAN, LTE-M, SigFox, and Narrow-Band Internet of Things (NB-IoT). Among them, LoRaWAN and NB-IoT are the two leading emergent technologies [24, 26]. To improve energy efficiency, NB-IoT combines the benefits of the 4G mobile network, namely the global coverage and the long-range, with the energy efficiency typical of LPWANs. Moreover, NB-IoT is designed to provide better indoor coverage and support of a massive number of low-throughput devices [27]. It is conceived to serve the high-value IoT market that pays for very low latency and high quality of service [28, 29]. In contrast, LoRaWAN is targeted to lower-cost devices, with very long-range (high coverage), occasional communication needs, and very long battery lifetime requirements.

NB-IoT is carried out over so-called "licensed" frequencies. These licensed frequencies refer to frequency bands in the overall spectrum that is regulated by a government entity, for example, the Federal Communications Commission in the United States. Examples of licensed frequency bands include those around 800 MHz for conventional mobile cellular telephony and those around 1.9 GHz for mobile PCS (Personal Communication Services). The licensing of frequencies allows those participants that have paid for the license rights to have private use of a particular licensed frequency band within a geographical area. This licensing minimizes the likelihood of interfering communications, permitting the exclusive licensee to control traffic in that vicinity, and to have recourse against unauthorized transmitters in those bands [30]. These license rights enable the license holders, such as wireless telephone service providers, to invest in mobile wireless communication infrastructures. Because of the license fees associated with licensed transmission and the investment in infrastructure, the licensed companies generally charge their customers for the use.

In the radio spectrum, unlicensed bands are also available. The "unlicensed" radio transmission in the unlicensed bands involves no license fees, so long as the transmitter respects specific regulations concerning the use of these allocated frequencies. An example of an unlicensed band is the instrumentation, scientific, and medical (ISM) band around 2.4 GHz. Current allocations of the unlicensed bands permit a large amount of bandwidth with no license fee, resulting in the deployment of many types of devices, such as wireless local area network (LAN) adapters and

access points, that provide high data rates (on the order of Mbps) and large spectral bandwidths (on the order of MHz). However, great plenty of interference from other unlicensed band users must often be tolerated.

Today, both NB-IoT and LoRaWAN are offering long-range and low power consumption with the primary aim of being employed as a wireless solution for IoT. However, to the best of my knowledge, there is no detailed comparison helping to select one of these two networking solutions given a specific application scenario. Although some characteristics of the considered technologies, such as the maximum range or the used bandwidth, are not directly comparable, there is a need for a thorough comparison in terms of QoS, deployment cost, and energy consumption.

The main objective of the second part of this Ph.D. Thesis is an experimental evaluation with in-field measurements of NB-IoT vs. LoRaWAN for IIoT applications. The comparison between the two protocols is performed in terms of power consumption, energy per bit, battery lifetime, and deployment cost. To have a realistic comparison, I use a WSN designed for Structural Health Monitoring (SHM). SHM allows evaluating the challenges mentioned above that are considered the primary obstacles for LPWAN deployments [31, 28]. Recently, several SHM solutions have been developed, such as crack meter based monitoring [32], and modal analysis [33].

The contribution can be summarized as follows:

- I present an accurate comparison between NB-IoT and LoRaWAN using experimental data from a real application scenario in 4.3;
- I validate the performance declared by communication protocols developers in realistic situations in 4.3;
- I provide guidelines for the selection and the deployment of the most suitable technology, based on the collected measurements and the current knowledge of the various solutions in Chapter 5.

The document is organized as follows. The primary MAC Layer Protocols for IoT architectures are described in Chapter 2. In chapter 3 introduces NETWIS (Wireless Inertial Sensors Network), the proposed system for motion capture. The sensor consumption patterns according to the different technologies presented and the life expectancy of the battery for the two configurations are presented in Chapter 4. Chapter 5 provides guidelines for the LPWANs deployment. Chapter 6 concludes the thesis.

Chapter 2

MAC Layer Protocols for WSN & IoT

Communication Protocols are the heart of IoT systems and enable network connectivity to high-level applications. Communication protocols allow devices to exchange information and data over the network. The protocols define the data exchange formats, data encoding, security mechanism, addressing schemes for devices, and routing of packets from source to destination. Other functions of the protocols include flow control, sequence control, and retransmission of lost packets.

Features such as coverage area, network topology, scalability, data transmission speed, installation costs, power consumption, transmission power efficiency, and delays are important issues for choice for using specific technology for a particular solution. In some circumstances, whenever we need to send big data over a wireless network, we do not have constraints for energy consumption. In other situations, we have small battery-powered devices that notify us of some occurrence, so the radio modules have to be as energy-efficient as possible. These choices have an impact on the whole project, especially on the Physical and Medium Access Control (MAC) level.

The objective of MAC is the creation of the sensor network infrastructure. The MAC scheme must establish a communication link between the sensor nodes and efficiently share the communication medium. Energy efficiency is one of the main aspects that must be considered. The sensor nodes are usually battery-powered, and it is often complicated to recharge batteries. Sometimes it is advantageous to replace the sensor node rather than recharging them. Energy efficiency can be increased by reducing energy wastage. Significant sources of energy waste in WSN are described in [34]. The throughput requirement varies with different applications. Some of the sensor network application requires to sample the information with precise temporal resolution. The latency requirement depends on the application. In some sensor network applications, the detected events must be reported to the sink node in real-time so that the appropriate action could be taken immediately. In many sensor network applications, when bandwidth is limited, it is crucial to guarantee that the sink node receives information from all sensor nodes fairly.

The purpose of this introductory chapter is to present an overview of the short and long-distance MAC level protocols used by IoT solutions, discussing the MAC

level features that define the behavior and applicability of each protocol. The section 2.1 presents two of the main MAC short-range coverage protocols, while long-range MAC level protocols are presented in 2.2.

2.1 Short Range

Short-range coverage medium access control (MAC) protocols are defined by the Institute of Electrical and Electronics Engineers (IEEE) as Wireless Personal Area Networks (WPAN), which is the network established between components that surround the human body.

2.1.1 Bluetooth IEEE 802.15.1

The IEEE 802.15.1 standard [35] is the basis for the Bluetooth wireless communication technology. Bluetooth is a low tier, ad hoc, terrestrial, wireless standard for short-range communication [36]. It is designed for small and low-cost devices with low power consumption. The technology works with three different classes of devices: Class 1, Class 2, and Class 3, where the range is about 100 meters, 10 meters, and 1 meter, respectively.

The main Bluetooth improvements, in the last release, include increased symbol rate, higher efficiency in the use of transmission channels on the 2.4 GHz band, and detection of interference and subsequent elimination.

The IEEE 802.15.1 MAC layer is composed of Logical Link Control, the Adaptation Protocol (L2CAP) layer, the Link Manager Protocol (LMP) layer, the Base-band, and the Radio. The Radio and the Base-band sub-layers define the Bluetooth physical layer. The Bluetooth MAC layer handles the communication types that can be asynchronous connectionless (ACL) or synchronous connection-oriented (SCO). Figure 2.1 shows the relationship between the IEEE 802.15.1 stack components.

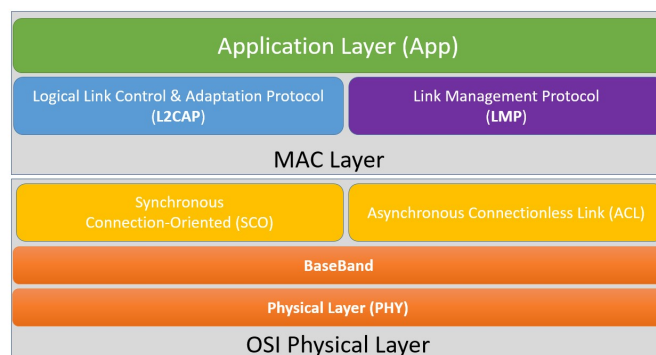


Figure 2.1: Bluetooth IEEE 802.15.1 Stack

The IEEE 802.15.1 radio operates in the 2.4-GHz Industrial Scientific and Medical (ISM) band using a short-range radio link and a fast frequency-hopping (FFH)

transceiver. The Bluetooth Radio layer provides the physical links among devices with 79 different Radio Frequency (RF) channels separated of 1 MHz, using a frequency hopping spread spectrum (FHSS) transmission method. This FHSS technique increases the robustness of the channel due to its capability to decrease the interference in the same frequency range. A Time Division Duplex (TDD) transmission scheme is specified to divide the channel into time slots of $625 \mu\text{s}$ each, corresponding to a different hop frequency, simulating full-duplex communication in the same transmission channel. A Link Management Protocol is a control protocol responsible for establishing base-band and physical layer links. The Logical Link Control and Adaptation Protocol (L2CAP) layer is a channel-based abstraction between the physical and service application layer. A pico-net cellular network is a group of up to seven slave devices, connected to a master device, which regulates the channel access. The master is responsible for managing the scheduling process messages to authorize a slave device to obtain the data transmission authorization.

2.1.2 Bluetooth Low Energie

Bluetooth Low Energie (BLE) was first introduced in 2010 to expand the application of Bluetooth for use in power-constrained devices such as wireless sensors and wireless controls that require low power consumption, amount of data transmission is small, and communication happens infrequently.

To address these different application requirements, BLE introduces a new radio, which is a derivative of the conventional Bluetooth and new interfaces. For BLE, the modulation scheme is GFSK with a raw data rate of 1 Msymbols/s with 2 MHz channel bandwidth, twice respect Bluetooth Classic. Due to the increase in channel bandwidth, there are a total of 40 channels in BLE: three advertising and 37 data channels, respectively. Since the robustness of the advertising channels is essential for setting up initial communications, they are chosen from channels that have less interference with Wi-Fi standards. The advertising channels facilitate discovering devices and establishing initial communication between two devices, which includes required parameter exchanges. Typically, a smartphone listens on these advertising channels, waiting for advertisement packets, sent by a device. Upon receiving an advertisement, the scanning device initiates a connection with a connection request packet. At this point, the advertising device becomes the slave, and the scanning device the master. After the connection is built, communication takes place in connection events, which occur at a period that can range from 7.5 ms to 4 s. The periods, called connection interval, can be changed even after a connection is established. At every connection event, the master transmits a packet to the slave, which may or may not respond. A BLE system uses a frequency hopping transceiver to combat interference between nearby devices.

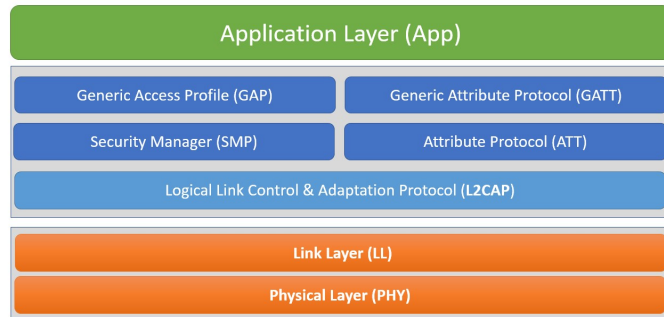


Figure 2.2: BLE Stack

Figure 2.2 shows the BLE stack. The host controller interface (HCI) isolates the controller part (link and physical layers) from the host part (Logical Link Control and Adaptation Protocol (L2CAP), Attribute Protocol (ATT), Generic Attribute Profile (GATT), and Generic Access Profile (GAP)). The PHY block is responsible for transmitting and receiving packets on the physical channel. The Link Manager is responsible for creating, modifying, and releasing logical links, communicating with other Link Managers on remote devices using the Link Layer Protocol (LL). L2CAP is the primary protocol at the link level. It deals with the multiplexing of data between different protocols of a higher level. Above the L2CAP layer, BLE is the application layer that uses a set of functionalities, which are not present in the Bluetooth Classic specifications. These blocks are the Attribute Protocol (ATT), the Generic Attribute Profile (GATT), the Security Manager Protocol (SMP), and the Generic Access Profile (GAP). SMP block provides the identification and encryption keys used in authentication procedures during device association. The ATT block implements the peer-to-peer protocol between an attribute server and an attribute client. The client opens the communication to the server on a remote device through an L2CAP channel. The Generic Access Profile block represents the basic features common to all devices Bluetooth, such as device role rights, discovery devices, and services, as well as establishing connections and security.

2.1.3 IEEE 802.15.4

The 802.15.4 standard includes the definition of the physical layer (PHY) and the Medium Access Control (MAC) sublayer for wireless connectivity. The devices involved can be mobile or fixed and often have stringent energy requirements. They are equipped with a battery because usually without access to the electricity grid.

IEEE 802.15.4 has some advantages: it is a flexible protocol stack, low cost, low energy consumption, reliable data transfer, and ease of operation [6]. The IEEE 802.15.4 standard architecture is defined through the concept of layers, which deal with the implementation of a specific part of the standard. Figure 2.3) represents these blocks graphically and how they are connected to the upper levels.

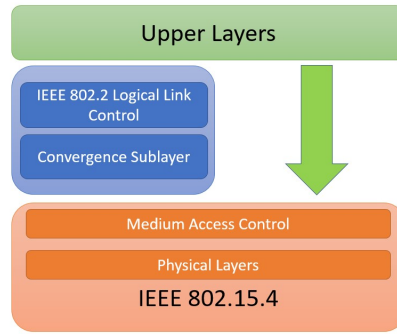


Figure 2.3: IEEE 802.15.4 Stack

The PHY Data Service allows the transmission and reception of PHY level packets, known as PHY Protocol Data Units (PPDU), through the radio channel. The access interface to the PHY Data Service is the PHY Data Service Access Point (SAP PD). Some of the features of the PHY level are the activation and deactivation of the radio transceiver, channel selection, Clear Channel Assessment (CCA), Energy Detection(ED), and Link Quality Indication (LQI). The access interface to the PHY Management Service is the PHY Layer Management Entity Service Access Point (PLME SAP).

Depending on the spectrum utilization of each region, according to the PHY layer specifications, the distances between IEEE 802.15.4 nodes can be up to 100 m. This range depends on propagation environment obstacles and the maximum transmission power levels defined by the IEEE 802.15.4 standard in the particular region [37].

2.2 Long Range

By 2020, more than tens of billions billion devices will be connected through radio communications in a big IoT world. In concomitance with the accelerated growth of the IoT market, low power wide area networks (LPWAN) have become an accessible low-rate long-range radio communication technology. LoRa and NB-IoT are two leading LPWAN technologies that compete for large-scale IoT deployment. These chapters provide a comprehensive and comparative study of these technologies, which serve as efficient solutions to connect smart, autonomous, and heterogeneous devices.

2.2.1 LoRa and LoRaWAN

Long Range (LoRa) is a proprietary spread spectrum modulation derived by Chirp Spread Spectrum (CSS) technique with integrated Forward Error Correction (FEC) developed by Semtech. The LoRa physical layer may be employed with any MAC layer; however, LoRaWAN is the currently proposed MAC that manages a simple star topology network. Long-range, high robustness, multipath resistance, Doppler

resistance, low power are the most important LoRa features. LoRa works in the lower ISM bands (EU: 868MHz and 433 MHz, USA: 915MHz and 433 MHz).

A LoRa radio transceiver has four configuration parameters: carrier frequency, spreading factor, bandwidth, and coding rate. The choice of these parameters defines energy consumption, transmission range, and robustness to noise [30]. A higher spreading factor improves the Signal to Noise Ratio (SNR), and consequently, sensitivity and range, despite also raises the air time of the packet. The number of chips per symbol is calculated as 2^{SF} . Each increase in SF divides the transmission rate and, hence, doubles transmission duration and energy consumption. The spreading factor can be selected from 6 to 12. Network separation using different SF is feasible because radio communications with different SF are orthogonal to each other. Bandwidth (BW) is the range of frequencies in the transmission band. Higher BW gives a higher data rate and shorter time on-air, but a lower sensitivity due to the integration of supplementary noise. A lower BW gives a higher sensitivity, but a lower data rate. Data is sent out at a chip rate equal to the bandwidth; for example, a bandwidth of 250 kHz corresponds to a chip rate of 250 kcps. Coding Rate (CR) is the FEC rate used by the LoRa modem and offers protection against bursts of interference. A higher CR offers more protection but grows time on air. Radios with different CR, stored in the header of the packet, and the same CF/SF/BW can still communicate with each other.

LoRa sensor network has some advantages. First, since the range is relatively broad (hundreds of meters indoors, kilometers outdoors), networks can span vast distances without routing over many hops. Moreover, transmission on the same carrier frequency, but with different spreading factor, are orthogonal. This creates the opportunity of dividing the channel into virtual subchannels. Finally, when transmissions occur at the same time with the same parameters, the most reliable transmission will be received with high probability. This feature is used by LoRaWAN, where all gateways broadcast beacon at the same time, and an end device can demodulate the most robust beacon.

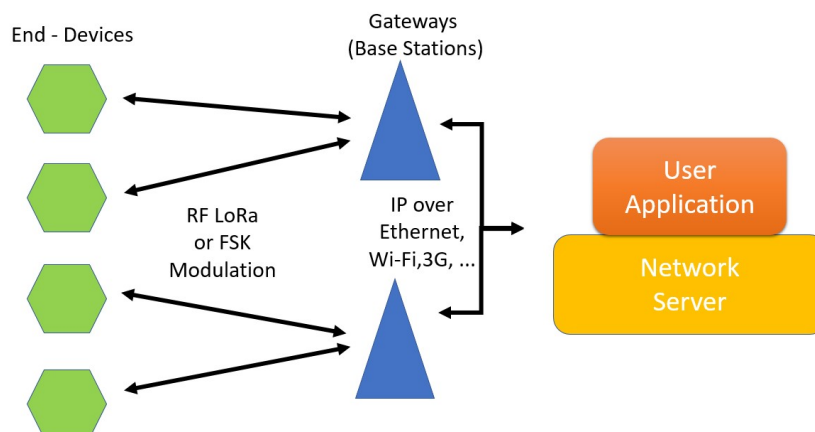


Figure 2.4: LoRaWAN Topology.

A LoRaWAN network consists of a star-of-stars topology composed of three fundamental elements: end-devices, gateways, and a central network server [38]. National standards regulate predefined channels. LoRaWAN specifications [38] establish ten different channels; the first nine have a bandwidth of 125KHz and support data rates between 0.3-5kbps. Channel ten is used to exchange messages with FSK (Frequency-Shift Keying) modulation and bandwidth of 250KHz.

ISO/IEC ISM regulations impose on each end-devices, working on ALOHA MAC (Medium Access Control) protocol, a limitation about the maximum duty cycle, which cannot exceed 1% of the channel time. However, as long as the restrictions for each band are respected, end-devices can transmit on different channels to increase their overall throughput [39]. They communicate with the network server through one or more gateways, which are also used to send downlink messages (Fig. 2.4).

The end-device uses the LoRa physical layer to exchange packets with the gateway, which communicates with the network server via an IP-based protocol stack.

There are three classes of LoRaWAN devices, called A, B, and C. Class A and Class B devices are usually battery-powered, while class C devices need to be supplied by the main due to the high energy consumption. The main difference in the three operating modes is the downlink connection, from the gateway to the device, which can be asynchronous in Class C and synchronous after the uplink, in Class A and B. Class A opens very short reception windows after sending a message, and then the device goes in a sleep state to save energy. Class B opens additional receive windows at scheduled intervals, using beacons sent from the gateway to synchronize the reception periods. Class C keep the radio in the continuous reception mode, allowing instant transmission of data. The different operating methods influence the power consumption and, consequently, the battery life of this device. The different operating methods influence the power consumption and, consequently, the battery life of this device. For example, in [40], authors show that Class C needs $225\times$ the energy used by Class A with static Spreading Factor (SF) and output power.

2.2.2 Sigfox

SIGFOX is an LPWA telecommunications network currently present in Western Europe, San Francisco, that allows two-way communication to and from the device. The SIGFOX network has been designed for sending small messages and only when they are needed. It is not suitable for broadband use (multimedia streaming). Energy efficiency features allow building network-connected devices that can last for years with a standard battery.

SigFox protocol stack consists of three principal layers: Frame, MAC, and Physical layers. Figure 2.5 shows the SigFox stack. The purpose of the frame layer is to receive the message originating from the upper layer, do the segmentation, and deliver the MAC layer the fragments generated. The MAC layer can identify and order the formation of the radio frames with a sequence number added. Moreover, the MAC layer header adds a field for device identification and error-detecting codes.

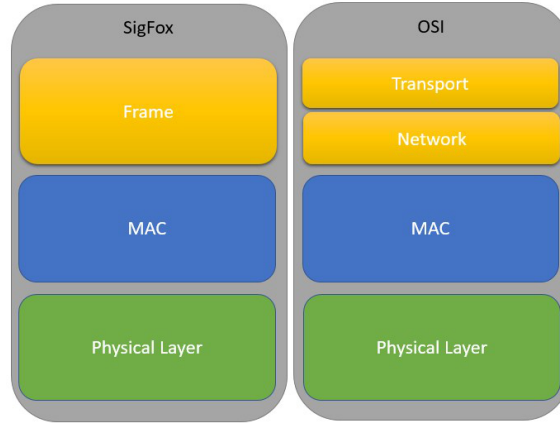


Figure 2.5: Sigfox protocol stack.

The SIGFOX network operates on sub-GHz frequencies, on the ISM bands: 868MHz in Europe and 915MHz in North America [41]. Sigfox is based on an ultra-narrow band (UNB) physical layer, where the binary data are broadcast with a differential binary phase-shift keying (DBPSK) modulation at 100 bps. Thus, the transmitted signal occupies a band of approximately $W_s = 100\text{Hz}$. The frequency hopping ensures channel diversity and deep-fading protection because it is done inside a bandwidth $B \gg W_s$ [42].

Sigfox nodes use a Random Frequency and Time Division Multiple Access (RFTDMA) to transmit their signals. The RFTDMA protocol allows active nodes to access randomly in time and frequency to the wireless medium without any contention-based protocol. The carrier frequencies are not chosen in a predefined discrete set, but inside a continuous interval B . Indeed, at the receiver side, the demodulator listens on the whole bandwidth B without recognizing a priori the carrier frequency used by the emitting device. The European legislation governing the 868 MHz bands allows a transmission cycle of 1%. A single device will, therefore, not be able to transmit for more than 1% of the time in an hour. Since the sending of a message can take up to 6 seconds, it follows that a maximum of 6 messages per hour and, therefore, 140 messages per day can be transmitted. Each message can be sent up to 3 times on different frequencies to improve reliability. Each message can contain up to 12 bytes for the application, also counting on a timestamp and a unique ID present at the message header level [43]. The completed packet structure is given below:

- a preamble (4 bytes)
- a frame synchronization part of 2 bytes
- a device identifier of 4 bytes
- a payload of up to 12 bytes
- a Hash code to authenticate the packet in Sigfox network (variable length)

- a Cyclic Redundancy Check (CRC) syndromes of 2 bytes for security and error detection

The bi-directional communication is performed when the transmitter asks it. In this case, it can mention that it is in listening mode until it receives data. In real propagation condition, Sigfox spans 50 to 100 of km distances and ensures to manage about 1 million devices per base station [44].

This claim is true until Sigfox does not coexist with other IoT technology. The work presented in [42], shows that the capacity to manage a million devices fades with the coexistence of a LoRa network.

Concerning the security aspects of SIGFOX networks, very few comments can be made as the SIGFOX protocols are proprietary and therefore closed. However, as a general approach, SIGFOX focuses on the network security itself, leaving the payload security mechanisms to the end users at both the transmitting side, that is, the SIGFOX node, and the receiving side, that is, the applications linked to the SIGFOX cloud via application programming interfaces (APIs).

2.2.3 NB IoT

NB-IoT is a novel protocol standardized by 3GPP [45]. It is also known as LTE Cat-NB1(NB2) and belongs to Low Power Wide Area (LPWA) technologies that could work virtually anywhere when infrastructure is present.

NB-IoT can coexist with GSM (Global System for Mobile communications) and LTE (Long-Term Evolution) under licensed frequency bands. NB-IoT occupies a frequency band width of 200 KHz, which corresponds to one resource block in GSM and LTE transmission [46]. It can operate in three different modes: stand-alone as a dedicated carrier, in-band inside the occupied bandwidth of a wideband LTE, and within the guard-band of an existing carrier (Fig. 2.6).

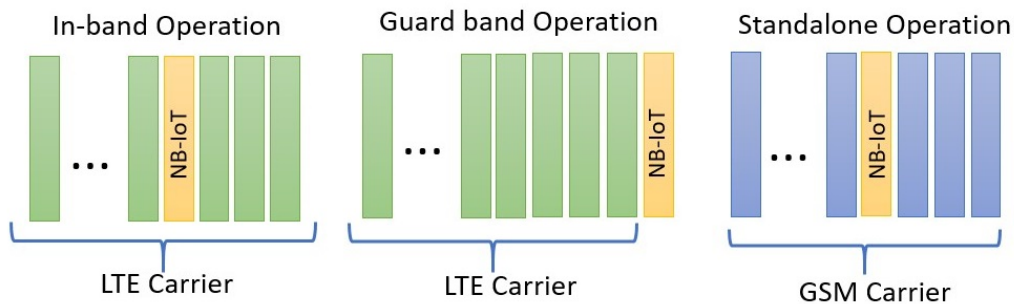


Figure 2.6: Operation modes for NB-IoT.

In the first deployment, NB-IoT can occupy one GSM channel (200 kHz) while for in-band and guard-band deployment, it will use one Physical Resource Block of LTE (180 kHz). NB-IoT uses the orthogonal FDMA in the downlink and single-carrier FDMA (frequency division multiple access) in the uplink and applies the

QPSK (quadrature phase-shift keying modulation) [46]. Each message can reach 1600 bytes of payload. The maximum data transmission rate is limited to 20 kbps for uplink and 200 kbps for downlink.

As discussed in [47], NB-IoT is designed for long-life devices and targets a battery life of more than 10 years when transmitting 200 bytes per day. To achieve these performances, NB-IoT uses the LTE energy-saving mechanisms, extending the timers period to minimize energy consumption. The features to decrease energy consumption are the connection release mechanism and the power optimization function, such as discontinuous reception and the power-saving mode. Communication requires a connection between the device and the network. This connection can be connected or Idle and is called RRC (Radio Resource Connection). First of all, when the device is woken up for the first time, the network connection is established, and the UE device enters in the RRC connected state. After, when the base station releases the connection, the device pass to the RRC idle state and stores the current access context. The device may later resume the RRC connected state with that context, thus avoiding considerable signaling overhead.

For devices with rarely uplink data transmission, and need to receive messages, power consumption can be reduced significantly by the eDRX feature, shown in Figure 2.7. Unlike the PSM mode, sending a message can be skipped, and a reception window is directly open. There are two ways for using this feature, Connected-eDRX or Idle-eDRX according to the state of the devices. When a device is connected, and there is no traffic, it alternates active listening and sleep periods. This behavior is maintained for the duration of the Inactivity Timer (Fig. 2.7). Otherwise, when a device is idle, new transmissions cannot be requested from the network, but the downlink channel is tracked at Paging Window (PW) events, to keep network synchronization and to discover if downlink data is pending. The time between two PW is the duration of an Idle-eDRX cycle (Fig. 2.7). For detailed information on eDRX see [48].

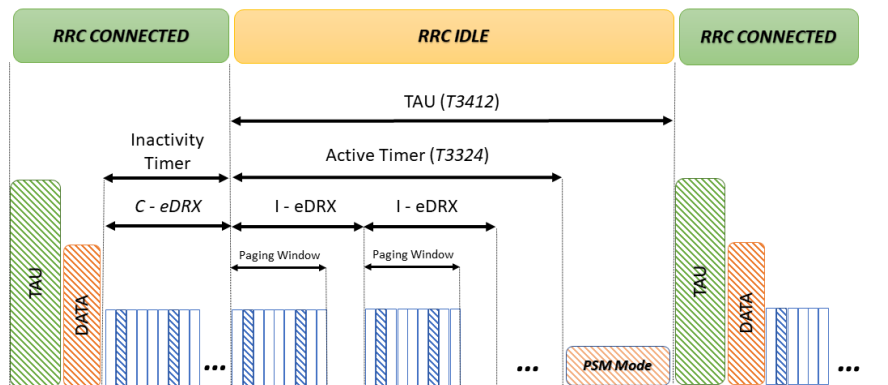


Figure 2.7: Extended Discontinuous Reception: the periodicity value of the reception windows can reach 10.24 s in Connected and 2.91 hours in Idle state, respectively. Power Saving Mode: device remains registered with the network, and it is not necessary to re-attach or re-establish the connection. The maximum duration of the PSM mode is 310 hours.

The PSM feature, shown in Figure 2.7 and defined in 3GPP Rel.12, is the deep sleep operation state. It allows reduction of the current consumption maximizing the amount of time that a device can remain in an extremely low power mode during periods of inactivity. After a wake-up, where data transmission generally takes place, it moves to the idle state, where reception windows are opened to allow downlink communication from the base station. The reception phase lasts according to the network policies agreed during registration. At the expiry of the timer T3324, the device switches in PSM. In this state, any receiving communication is disabled, but the device remains registered on the network, and re-joining is not necessary when it switches back to transmit. The PSM mode disconnects the radio entirely so that the device can enter deep-sleep. However, the device can resume the connection at any time. In order to inform the network that the device is still alive, the T3412 timer is configured so that the device wakes up periodically to perform a tracking area update (TAU). The TAU can be configured with a more extended period of up to 413 days for NB-IoT.

2.3 Conclusion

There are many wireless technologies in the IoT network, each one has certain specifications and benefits. Each application must be precisely defined at the design stage, in order to understand which technology provides the most guarantees for meeting the requirements.

Classic Bluetooth offers higher throughput and bandwidth, which makes it suitable for data stream applications (audio and video streaming). Nevertheless, it has several limitations, including a limited number of nodes in the network (up to seven slaves) or topology. BLE is a significant improvement in respect to Bluetooth classic for IoT application. The advantages include lower power consumption, lower setup time, and supporting star network topology with an unlimited number of nodes [49, 50]. The several comparisons between BLE and IEEE 802.15.4 clarify the lower power consumption of BLE against IEEE 802.15.4. However, the PHY layer of the standard IEEE 802.15.4 is used as a base for many other short-range protocols citeoliveira2019mac. Moreover, it allows a wide transmission range, depending on the output power.

Various factors have to be considered to choose an appropriate LPWAN technology for an IoT application: QoS, range, device lifetime, payload length, deployment, and cost.

Sigfox and LoRaWAN employ license-free sub-GHz bands and asynchronous communication based on ALOHA protocol. NB-IoT employs licensed spectrum and LTE-based synchronous protocol, which are optimal for QoS at the disadvantage of cost. LoRaWAN has a lower range (range <20 Km) than Sigfox (range >40 km). NB-IoT has the lowest range (range <10 Km). The NB-IoT end-device spends additional energy due to synchronous communication and QoS handling. This additional energy consumption reduces the NB-IoT end-device lifetime compared to Sigfox and LoRaWAN. The NB-IoT standardization was published in 2016 and is actually under rollout to install its network over the world. On the contrary, LoRaWAN and Sigfox technologies are mature and under commercialization in various

countries and cities. Various cost factors should be considered, including spectrum (license), deployment, and end-device costs.

Chapter 3

Wireless Inertial Sensors Network

3.1 Body Sensor Networks

BSNs are WSNs that focus on the monitoring of the human body [17] using wearable sensors nodes. Wearables, which can collect data in aggregate form, are used primarily for information about general well-being but not for making decisions about one's health.

Although BSNs are a sub-family of WSN, the majority of BSNs adopts star network topologies, where the central node is often the bridge to a wired system [51], while WSNs are inherently multi-hop. The WSNs generally have a wider range of operability and have a much higher number of nodes. The BSN number of nodes is typically less than ten units because it would be disturbing for the user to wear a higher amount [52]. Moreover, they have more stringent requirements in terms of size and weight than WSN nodes. Those constraints reduce the energy availability since the batteries of the BSN nodes need to be small. On the other hand, BSN typically requires a higher variables sampling rate, in the order of dozens Hz, than physical quantities of WSN, such as temperature, humidity [53].

Another challenge of a BSN, compared to traditional wireless systems, is that the communication channel is strongly influenced by the proximity of the human body, which attenuates the transmitted signal and affects the field distribution around it, due to the scattering from different surfaces. Moreover, the presence of human tissues close to the antenna may cause detuning and pattern distortion effects. Therefore, to design a reliable and efficient BSN, proper analysis and modeling of the radio channel, including the human body and the plastic case of the devices are required.

3.1.1 BSNs Applications and Open Issues

The most popular application for BSN is mainly e-health to monitor and support patients with pathologies [53, 54, 55, 56] and for fitness/sports activities monitoring [57, 58]. Applications related to body movement reconstruction, are the most critical in terms of data rate and robustness, as the sampling rate of the various inertial/motion units (IMU) is in the range of 60 Hz, and must be precisely synchronized (error less than 1 ms) for real-time reconstruction. In recent years, multisensor data fusion

has received significant attention: in the BSNs, cooperative sensor fusion is the most common. Multiple sensor signals are needed to obtain information that could not be achieved by looking at any of these signals independently [59]. Data fusion techniques combine data from multiple sensors, to achieve improved accuracies and more specific inferences than could be achieved by the use of a single sensor alone [60]. In these applications, generally, all information is sent from the end devices to an intelligent unit, which interprets the variables, calculates the data of interest, and makes the necessary decisions. This approach congesting the communication band when the number of nodes increases. For these reasons, the volume of collected data has grown [60, 61].

Xsens MVN is a motion capture system available in specific versions to accommodate consumer needs. It uses wireless motion trackers (MTw) and body straps. Data is transmitted wirelessly between each motion tracker at 60 Hz [62]. It has been demonstrated that 60Hz frequency is sufficient for reliability scenarios [63, 64]. Each MTw (size 47 mm x 30 mm x 13mm), weighs 20 g [62].

3.1.2 Goals, Challenges and Insights

The majority of wearable devices were only collecting raw data from the sensors without processing them. One of the technology challenges is information transport from a multitude of elements present in the environment up to a gateway, which makes this information available for aggregation and processing of the highest level. This need to have all this information saturates the available band, typically limited, due to the typically high number of devices. On the contrary, processing of the quantities of interest directly in the local area decreases the bandwidth required on the communication channel. These nodes must have the computational capacity to perform sensor-fusion algorithms locally for the sensor orientation calculation relative to a fixed reference system in space [65].

The goal is to create a BSN that exploits a dual-core Inertial Measurement Unit (IMU) for sensor fusion. Local sensor fusion algorithms on IMUs can employ the core at the highest computing power with ARM Cortex M4. The other core, used for wireless transmission, implements a customized TDMA protocol IEEE 802.15.4 based, which is responsible for keeping the network synchronized. The objectives of the protocol are to maximize throughput and minimize packet loss. Moreover, onboard processing is energy efficient and enables a real-time decision given feedback at the user with low latency [66, 67, 68, 69]. Furthermore, a customized gateway unit has been designed to transfer network data via USB.

Finally, this scenario, with the power supply constraint, involves optimizing operating modes by switching off units at non-use moments in order to conserve energy. These features should not be to the detriment of user experience, so the final device will have to be as compact as those currently on the market and have a time of use sufficient to the task required. The goal is obtainable, thanks to the improvements obtained in the microcontroller world regarding the dissipated power and the miniaturization of packages. As the local performance increases, it will be possible to do processing directly, reducing the bottle's neck due to protocols and obtaining more precise data thanks to the calculation performance of new architectures. The

proposed system can be replaced with the one used in [56, 59, 16, 62].

3.2 System Architecture

NETWIS consists of several wearable Wireless Inertial Sensor devices (WIS) that communicate to a single gateway (GW) connected to a central unit, in a star topology network. The gateway, in addition to the wireless interface, can communicate via USB to a high-level application. One of the primary goals of designing NETWIS was to maximize the effective throughput of the whole system.

Fig. 3.1 shows the high-level system architecture of the proposed approach. The various inertial units are placed in the points of interest of the patient's body and communicate with the GW unit connected to the computer. High-level applications resident on a PC, e.g., multi-sensor fusion algorithms [60], can manage nodes in real-time.

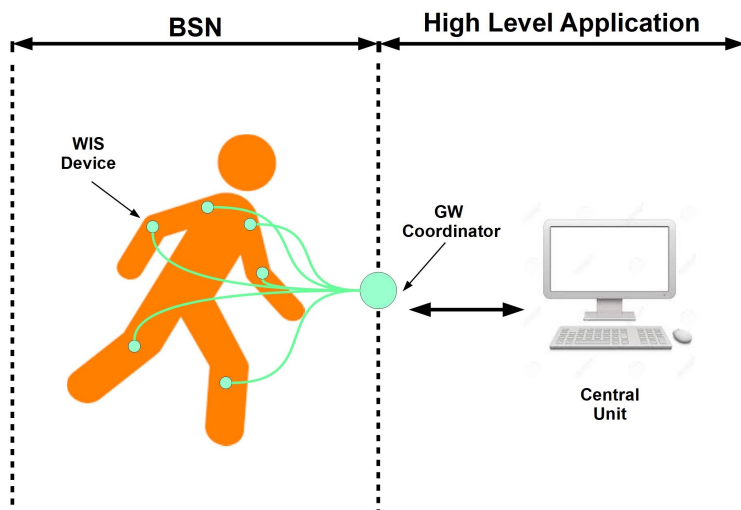


Figure 3.1: Overview NETWIS system: several WIS devices communicate the data acquired to the high-level application via the GW, a central node in a star network.

The communication methods and transmission times are managed by the GW, which is the master of the star network. The user is free to move around the unconfined area for a radius of 30 meters in an open field. The system allows the execution of motion tracking algorithms based on the data sampled by the gyroscope, the magnetometer, and the accelerometers on WIS devices.

The developed system has been designed to satisfy the following main requirements:

- Computational capability: calculation of quantities such as quaternions and spatial coordinates directly on the WIS, by the execution of Kalman filtering on signals from accelerometers, gyroscopes, and 3D magnetometers. Many Motion Capture solutions have been developed based on Kalman filters [70, 71].

In the Kalman filter, the measurement equations are applied to improve the estimation of the states with the aid of the sensor outputs. The Kalman filter is an efficient recursive filter that evaluates the state of a dynamic system, starting from a series of measurements subject to noise. Due to its intrinsic characteristics, it is an excellent filter for noises and disturbances acting on Gaussian systems with zero mean. The key practical issue in nonlinear filtering is computational complexity [72]. The work [73] shows how the computational complexity of the different Kalman filters implementation in terms of FLOPS (FLoating-point Operations Per Second). Based on this, the system computes units must have a Floating Point Unit available.

- Scalability: flexible nodes number according to the application, up to 20 units. The proposed system must be flexible in terms of the number of nodes and associated frequency respected other solutions [62].
- Data rate: sending of the filtered data of accelerometers, gyroscopes, and magnetometers in radio packages with a frequency above 60 Hz.
- Synchronization: the synchronization error must be less than 1 ms to optimize multi-sensor fusion on the high-level application.
- Lifetime: the battery should have dimensions less than 10 x 25 x 40 mm and must last at least 3 hours; the battery charging is made via a wired connection.

3.3 Hardware Implementation

This section illustrates the hardware implementation of the proposed system. A fundamental requirement for any wearable design will be the use of an "always active and always aware" processor to manage the continuous monitoring of sensors such as accelerometers and gyroscopes, global positioning devices. The processor must handle increasingly sophisticated algorithms and perform "sensor fusion" by filtering and interpreting the data of all these sensors to provide better information to the user. A powerful 32-bit processor core will be needed to maintain all the processing on the chip, thus reducing the amount of data transmitted and keeping energy consumption to a minimum [74].

ARM is the world leader in developing advanced technologies for mobile and wearable devices, providing an extensive assortment of processor and other SoC (System-on-Chip) Intellectual Property (IP). Based on this IP, SoCs from ARM partners have encouraged hardware developers to adopt wearable device platforms based on ARM that can immediately address this massive base of consumers. In conjunction with world-leading semiconductor partners, ARM is, therefore, well-positioned to apply its expertise in low-power mobile technologies and play a leading role in the creation and development of wearable products.

The Cortex-M series has become an industry standard, with more than five billion Cortex-M processors shipped to date. It ranges in terms of power consumption from the ultra-low-power Cortex-M0+ up to the top-of-the-range, high-performance Cortex-M4 core. This high-end core offers highly efficient signal processing features

The Cortex-M4 raise performance to 3.40 CoreMark/MHz with powerful digital signal processing (DSP) instruction set and floating point capability provides the computing performance needed for the wearable and IoT worlds.

Table 3.1: CoreMark and Dhrystone per MHz performance benchmarks for the ARM Cortex-M series (Courtesy of ARM).

	Dhrystone	Dhrystone (opt.)	CoreMark
<i>Cortex M0</i>	0.87	1.27	2.33
<i>Cortex M0+</i>	0.95	1.36	2.46
<i>Cortex M3</i>	1.25	1.89	3.32
<i>Cortex M4</i>	1.25	1.95	3.40
<i>Cortex M7</i>	2.14	3.23	5.01

For these reasons, considering the complexity of the algorithms used for motion tracking, I believe that the choice of a microprocessor with an M4 core is essential.

The K22 MCUs family has been optimized for cost-sensitive applications requiring low power flexibility and processing efficiency thanks ARM® Cortex®-M4 core + DSP at 120 MHz. Moreover, to minimize power consumption, it has ten low-power modes and a Low-leakage wake-up unit [77].

The Kinetis KWx1Z MCUs family combines a 2.4 GHz transceiver supporting FSK/GFSK and O-QPSK modulations, an Arm® Cortex®-M0+ CPU, up to 512 KB Flash and up to 128 KB SRAM. The KW41Z is a solution for single-chip designs that need coexisting communication on both a Bluetooth Low Energy network and an 802.15.4 based network. Initially used for automation and healthcare purposes, these MCUs enable low-energy and long-range connectivity. Smaller size (7x7 QFN package) and low component count reduces cost and areas [77]. In the Figure 3.4, we see an image of the realized prototype.

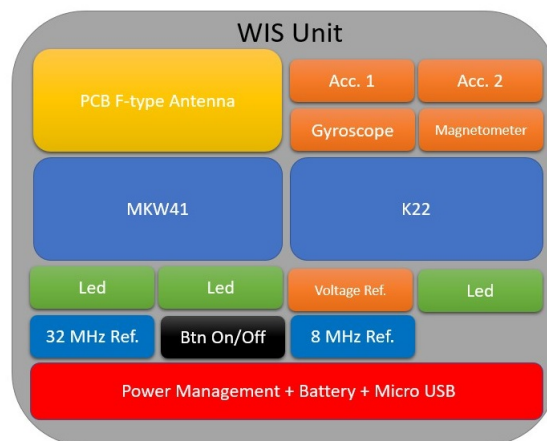


Figure 3.3: Blocks diagram WIS unit: the dual-core platform incorporates a digital magnetometer, a gyroscope, and two analog accelerometers.

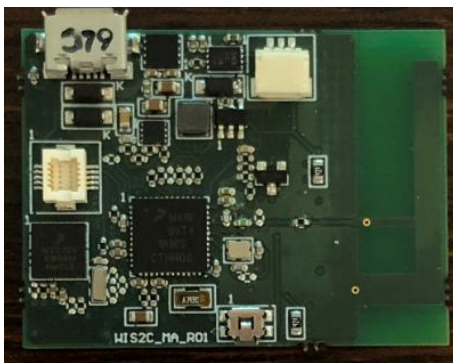


Figure 3.4: WIS unit: the dimensions are 40 mm x 30 mm, the weight is 20 g.

3.3.2 Gateway

The GW unit, Kinetis KW24D wireless MCU based, provides a low-power, compact device with integrated IEEE 802.15.4 radio, targeting control and monitoring applications [77].



Figure 3.5: Blocks diagram GW unit.

The integrated USB Full Speed driver makes it ideal for high throughput to a PC, while programmable power output up to + 8 dBm is useful for varying distances in different indoor and outdoor applications.

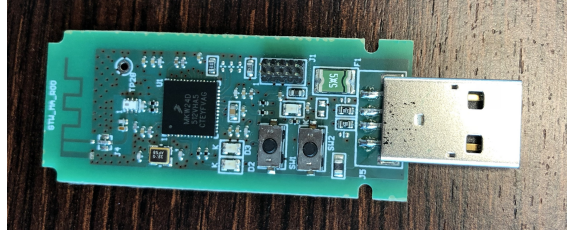


Figure 3.6: GW unit: the dimensions are 80 mm x 20 mm.

3.4 Antennas Analysis

There are several antenna types to choose from when deciding what kind of antenna to use in a wireless IoT product. Area, cost, and performance are the most important factors when choosing an antenna. The three most commonly used antenna types for short-range devices are PCB antennas, chip antennas, and wire antennas. The PCB antenna provides superior performance and reduced production costs. Furthermore, the simulations allow evaluating the effects of detuning due to the case to the patient's body and the metal objects. A detailed study of the pros and cons of the various solutions is available in [78].

An essential part of the project was an accurate analysis to find the best compromise between the costs, the spaces, and the performance of the antennas of the two devices. In summary, I focused on applications such as instrumental analysis of patients for rehabilitation purposes in indoor environments, in rooms without significant obstacles. A typical case could be short distances up to 15 meters to monitor movements during a walk. Outdoor uses are sporadic but possible, however, considering maximum distances of 30 meters. The communication protocols taken into consideration are IEEE Standard 802.15.4 and Bluetooth Low Energy (BLE).

In designing a wearable device, the main issues to be addressed are:

- Detuning effects of the antenna due to the patient's body.
- Small size to reduce encumbrance (need to wear more devices).
- Possible interferences between different devices.
- Battery-powered: reduced power consumption to increase battery life.
- Minimized radiated power to reduce patient SAR (Specific Absorption Rate).

To sum up, the goal is to respect the range specifications (15 meters indoors, 30 meters outdoors) while simultaneously guaranteeing the minimization of transmitted power and minimizing dimensions. Factors that influenced the choice are:

- Application frequency and bandwidth.
- Margin in the link budget.
- Antenna positioning: polarization, directivity, near-field interactions.

- Simulation / optimization skills.
- Weight, cost, bulk.

3.4.1 Antenna Selection

Considering that wire, loop and whip antennas are to be excluded as they do not bring advantages at 2.4 GHz, the PCB and antenna chip solutions remain. The antenna chips are very compact, have a fast time to market and lower development costs. However, they have less gain and less efficiency of the PCB antenna, little possibility of tuning/optimization to the specific design. On the other hand, the PCBs antenna has an almost negligible production cost, more significant gain (+ 3dB) and higher efficiency (+ 20%) than the chip antenna. Moreover, they have the possibility of tuning/optimization to the specific design. Both types have an omnidirectional radiation pattern.

In conclusion, the PCB antenna was chosen. Having electromagnetic simulation (EM) capabilities, this antenna type provides superior performance, reduced production costs, and a more excellent uniformity of performance [78]. Furthermore, EM simulations allow the antenna optimization in the function of the board in which it is housed and the evaluation of detuning effects due to the envelope, to the patient body, and metal objects present.

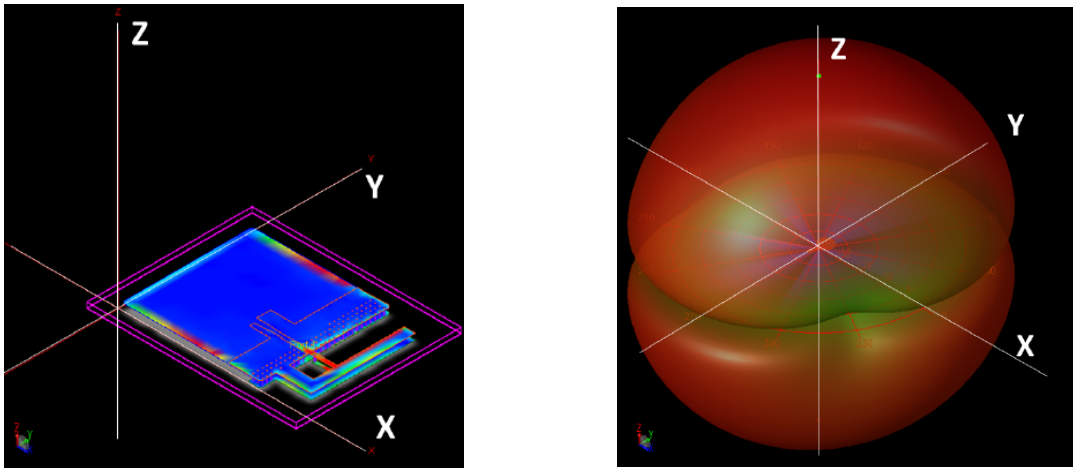


Figure 3.7: Omnidirectional antenna diagram except for two minima at theta near $+ 90^\circ$ and -90° degrees. It is necessary to avoid the antennas orientation that involves the direction of the connection in correspondence with these minima.

In particular, for the minimization of the space, it was chosen for a monopole PCB antenna of the PIFA type (Planar Inverted F Antenna). In the simulation phase, the jig was measured to evaluate the loading effects of the patient's bbody and to synthesize the best adaptation network (inductance and capacitance) between RF transceiver and antenna. The best connection between the devices occurs when the gateway and the sensor PCBs are on the same XY plane and perpendicular to the XZ plane of the floor. On the contrary, the minimum range condition occurs when the sensor PCB is on a plane perpendicular to that of the gateway PCB.

3.4.2 Link Budget

The factors that mainly influence the range of the wireless system are the transmitted power, the sensitivity of the receivers, the gains and the adaptation of the antenna, the multipath/fading phenomena, and the possible interferences.

Table 3.2: Link Budget

	USB-KW24D512 (GW)	MKW41Z (WIS)
Pout max	8 dBm	3.5 dBm
Sensitivity (IEEE 802.15.4)	-101 dBm	-100 dBm
Sensitivity (BLE)	-	-95 dBm

The GW always operates at a power exceeding five dBm considering it is powered by USB from a PC. Two communication scenarios are provided: IEEE 802.15.4 and BLE (for each indoor and outdoor). In the BLE scenario case, since there are no data on the operation of the gateway with this protocol, the sensitivity is considered to be the same as the sensor node (-95 dBm). For the indoor scenario, two cases are considered: poorly furnished office (indoor 1) and very furnished (indoor 2), which correspond to additional losses 10 dB and 21 dB, respectively. Other hypotheses considered are 1.5 meters high of the gateway, sensor positioning height variable from 0.2 to 1.5 meters, absence of other interfering signals, and optimal orientation between the antennas. With the term range, I identify the section from the sensor to the gateway.

Table 3.3: IEEE 802.15.4 - Tx Power set = -15 dBm

H sensor (m)	Outdoor(m)	Indoor 1 (m)	Indoor 2 (m)
0.2	84	40	15
0.4	100	49	15
0.6	114	54	14
0.8	127	54	15
1	139	54	15
1.2	149	54	15
1.5	163	42	16

Table 3.4: IEEE 802.15.4 - Tx Power set = -9 dBm

H sensor (m)	Outdoor(m)	Indoor 1 (m)	Indoor 2 (m)
0.2	130	62	28
0.4	151	75	31
0.6	171	86	31
0.8	189	96	31
1	206	104	24
1.2	222	107	27
1.5	243	107	30

Table 3.5: IEEE 802.15.4 - Tx Power set = -3 dBm

H sensor (m)	Outdoor(m)	Indoor 1 (m)	Indoor 2 (m)
0.2	203	96	44
0.4	229	113	54
0.6	255	129	62
0.8	280	144	62
1	304	157	62
1.2	326	168	62
1.5	356	184	62

Table 3.6: IEEE 802.15.4 - Tx Power set = 0 dBm

H sensor (m)	Outdoor(m)	Indoor 1 (m)	Indoor 2 (m)
0.2	253	119	55
0.4	282	139	66
0.6	313	158	76
0.8	342	175	85
1	369	190	87
1.2	395	205	87
1.5	432	225	87

3.5 Wireless Communication Protocol

In this section, I present NetWIS, the middleware developed in this work, positioned between the application and the MAC layers. The firmware has been designed to maximize the scalability and throughput and minimize the synchronization error with several WIS nodes.

The SMAC stack implements the Medium Access Control (MAC) layer. The participating agents will be of two types:

- 1 Gateway (GW)
- N Wireless Inertial Sensor (WIS)

The following parameters characterize a generic network: the WIS unit number (N), the data update frequency requested by the GW ($f_{refresh}$), the channel availability time for every node (T_{Slot}), the IEEE 802.15.4 channel selected, the operating mode (Simplex, Medium, Raw).

In order to optimize the consumption of the network units, the communications must take place at particular time intervals called Communication Rounds (Fig. 3.8).

$$T_{Update} = \frac{1}{f_{refresh}} \quad (3.1)$$

T_{Update} is linked to the required refresh frequency ($f_{refresh}$), as shown in equation 3.1.

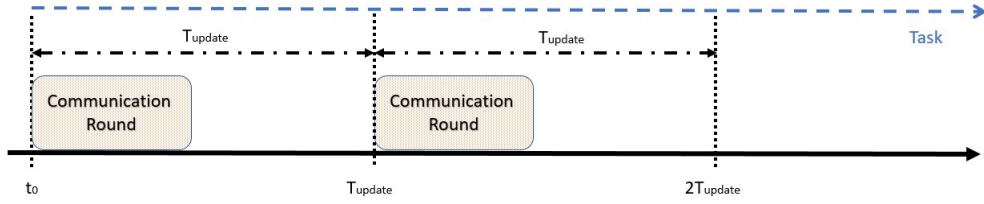


Figure 3.8: Communication Round.

Each node of the network must be able independently to determine the time to send its information content. The sending will be carried out through a periodic interrupt routine. As shown in figure 3.9, the GW must transmit at the start of each communication round, in slot 0, depending on the timer expiration. The time that elapses between a sending and the following one must be less or equal to the frequency of updating the data of the PC $f_{refresh}$. After the GW, the other units of the network will respond, each in its assigned slot.

Outside of these precise slots, the devices can turn off their radios, in order to reduce energy consumption, as there are no messages on the network.

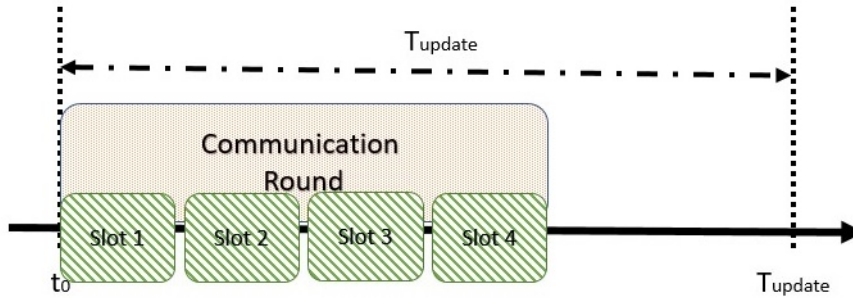


Figure 3.9: T slot.

The WIS units must configure themselves according to the transmission frequency required by the GW and the total number of units in the network. The synchronization of the nodes will be managed by the central host, which will coincide with the GW. The slot assigned to the GW will always be the first, in which it will send the synchronization information to all end-devices in a broadcast mode. The other slots are pre-assigned according to the ID of the WIS saved in internal flash. The GW, at global time 0, will send the first packet of the network.

In addition to the band, the project added value is to obtain the maximum synchronization among the nodes, so that the data processed by the application is aligned as much as possible for the overall movement reconstruction. The protocol is based on this constraint, forcing the acquisition and calculation of units at the same time.

There are several stages of operation. The preliminary phase of the system concerns only the GW, which determines the channel according to appropriate policies.

The GW may have arbitrarily chosen it, through an analysis of the frequency spectrum of the environment, or could be set by PC according to the user's preference. After that, every task managed by NETWIS splits into "Setup" and "Working" phases.

- SETUP: the GW configures the individual units according to the parameters received.
- WORKING: the units send the information calculated according to the set mode.

3.5.1 Setup Phase

The nodes must be connected to the GW on an unknown channel a priori (Fig. 3.10). Setup is divided into two sub-phases, which alternate consecutively until the configuration message reaches all the enabled nodes of the network.

- Channel Broadcasting.
- Channel Acknowledgement.

In the Channel Broadcasting phase, the GW sends a broadcast message with the configuration information on the selected channel. The WIS cycle on all possible channels until they receive the message. Only one WIS must reply to this message, the one to which the address in the payload of this message refers.

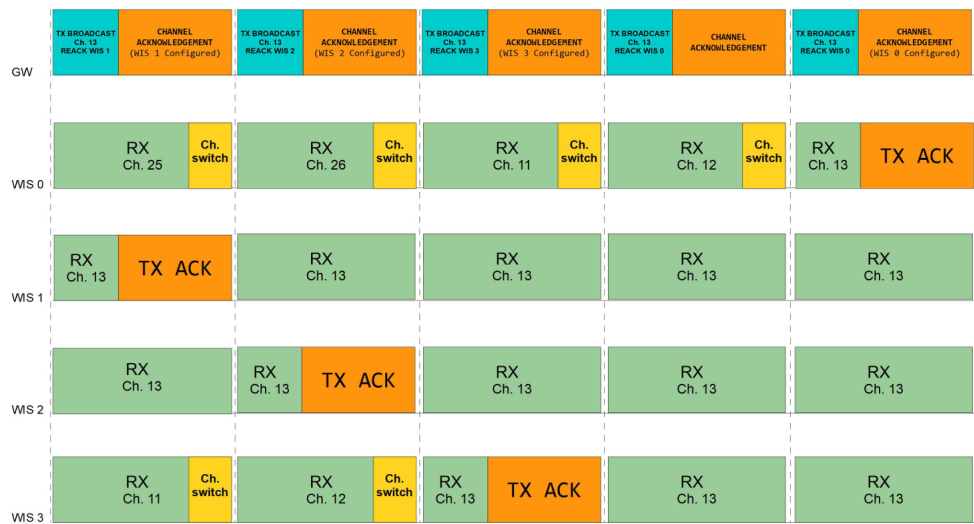


Figure 3.10: Bootstrap: the nodes must be connected to the GW on an unknown channel a priori.

In the Channel Acknowledgement phase, the GW waits for the response of the WIS that it had indicated in the last message transmitted. The WIS configured correctly responds with an ACK, NAK, otherwise. The average configuration time is 179,8 ms in the case of a network with a single WIS, while it rises to 219,8 ms with five units.

3.5.2 Working Phase

In this phase, the units send the calculated information, using sensor fusion algorithms (out of thesis), according to the operating mode set.

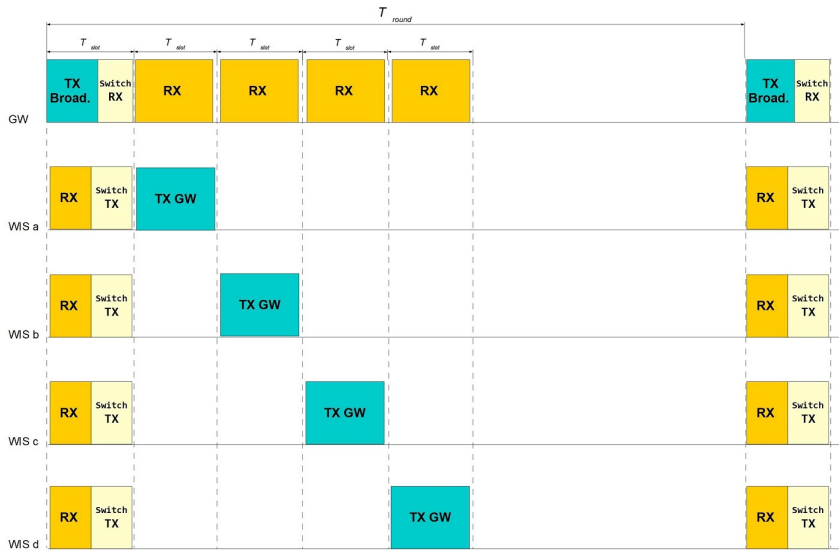


Figure 3.11: Scheduling in NETWIS with five nodes: the T_{round} is the reciprocal of the WIS sampling rate set by the GW. The slot time T_{slot} can be set up to 5 ms. For transmission of a 19 bytes message, 1.5 ms is sufficient in practice.

The protocol type is Time Division Multiple Access (TDMA). The NETWIS basic principles are mainly the "Shared Bus" infrastructure, where each node transmits in a predetermined slot ([79]), and the time-triggered communications. Each node in the network must be able to determine the time it takes to send its information. This mechanism uses a normal interrupt routine. The GW must always transmit in the first slot, depending on the expiration of one of its timers. After that, the WIS units send each one in the corresponding preassigned slot the same message type. The message of the GW, sent in broadcast, synchronizes all the WIS. Thanks to the Setup Phase information received, these know how to configure themselves to transmit in the allocated round. The various processes described above are represented in Fig. 3.11.

On-board operations must also be synchronized. In the example of Fig. 3.12, we have a generic WIS_i during the working phase. Let us examine the moment where a generic m -th acquisition of the data from the sensors is scheduled. The GW, via broadcast request, synchronizes the micro KW_i , which wakes up the micro K_i by

wake up command. Once active, the micro K_i sends the previously calculated data for the next wireless transmission. The latency of the protocol for a given m -th data is always smaller three times $f_{refresh}$ (equation 3.2).

$$2 \times \frac{1}{f_{refresh}} < Latency < 3 \times \frac{1}{f_{refresh}} \quad (3.2)$$

The GW synchronizes the sampling of quantities and the following sensor fusion algorithm. Once the algorithm is executed, the micro K_i returns to idle until the subsequent request. Note that it is not necessary for the algorithm to have a fixed duration, the only constraint is that it is less than the T_{round} (the needed time for serial communication is negligible).

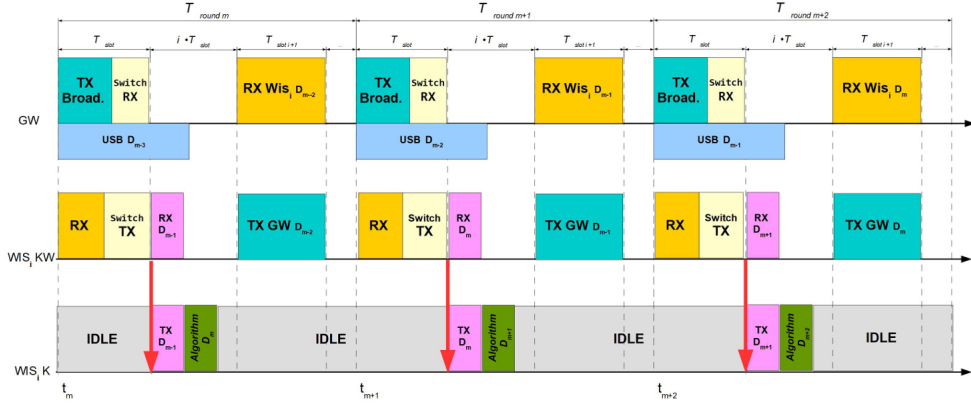


Figure 3.12: Dual-core operations: unit K_i is woken synchronously when the broadcast message is received on the KW_i . In this way, all the network units remain aligned.

3.6 Firmware Implementation

3.6.1 SMAC

SMAC is the lowest cost solution that can be used in NXP transceivers and systems-in-package like MC1319x, MC1320x, and MC1321x. It supports star and peer-to-peer networks, but more sophisticated approaches can be developed, creating a network layer or adding repeater nodes. It is written in full ANSI C. SMAC implements neither the full stack of ZigBee nor the full 802.15.4 level, but it is a simple and easy to use protocol.

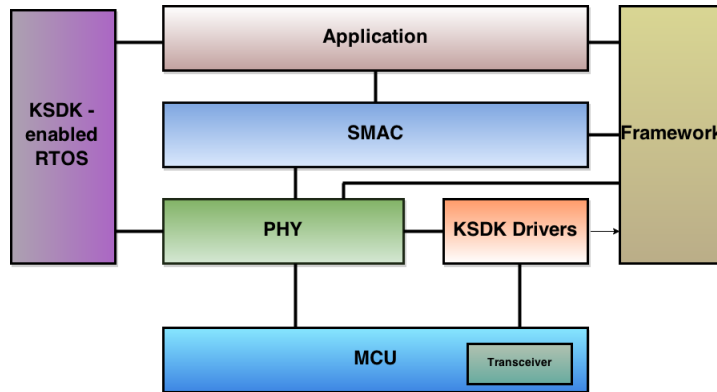


Figure 3.13: SMAC Architecture

Low-cost applications that require basic primitives, like transmission, reception, and power and channel selection, are good examples of what SMAC can do [80]. The typical uses of this stack are cable replacement and remote control. Mainly, SMAC can be described as a driver between the transceiver and the MCU. It also includes functions to initialize the MCU and peripherals, such as serial communication interface (SCI), plus the security and the over-the-air-programming (OTAP) modules.

The SMAC layer is the connection between the application and the SMAC core. Some of the most important primitives of the SMAC include:

- **Transmission:** `MCPSDataRequest` is a blocking function used to transmit packages. The users must provide a pointer to a previously created packet.
- **Reception:** `MLMERXEnableRequest` and `MLMERXDisableRequest` are used for enabling/disabling the transceiver for a reception. A timeout parameter can be passed to this function to wait for a reception for a fixed time length. `MCPSDataIndication` is a callback function executed each time a packet is successfully received, or a timeout occurs. It is recommended that this is executed as quickly as possible since this function is executed inside an interruption.
- **Energy Measurement and Managemen:** `MLMEEnergyDetect` and `MLMELinkQuality` can be used to estimate the channel energy in decibels (dBm) before and after packet transmission. The users can use these primitives to create a clear channel assessment (CCA) algorithm and a procedure to efficiently determine how many dBm is required to transmit to a nearby device. `MLMEMC13192PAOutputAdjust` sets the power used by the transceiver to transmit a packet. It can be changed at any moment.

The essential reason for choosing this solution is the maximum number of nodes, compared to other stacks it provides significantly higher scalability [17] requested by interested application [53].

3.7 Experimental Results

To evaluate the functionality and the performance of the proposed system, in particular, the scalability and the maximum achievable throughput, I realized and developed both the WIS node and a GW, and I deployed them on the field. The following subsection presents the gained experimental results.

3.7.1 Throughput and scalability

As a first step, I have empirically measured the data rate, with SMAC protocol, of a generic end device that sequentially sends an identical message. This value varies greatly depending on the length of the payload, considering that SMAC has a constant overhead.

I measured that for small packages (19 B, including the 9 bytes of SMAC overhead), it does not fall below 115 Kb/s. Regarding SIMPLEX mode, where each message is 19 B, the send time is 1.32 ms. Setting a T_{Slot} equivalent to 1.5 ms, I increase the ideal transmission window of 12%, ensuring that I eliminate any overlapping between the nodes of the network due to synchronism errors.

Through this empirical assessment, I identify the condition of the existence of potential instances of NETWIS networks. I indicate with T_{GW} the maximum time to send the GW message (and the complete WIS message processing), T_{WIS} the maximum time to send WIS message (and the end GW message processing). By defining a configuration such as the $N, f_{refresh}$ pair, under the Simplex mode hypothesis, I have that:

$$T_{GW} + T_{Wis} \times N < \frac{1}{f_{refresh}} \quad (3.3)$$

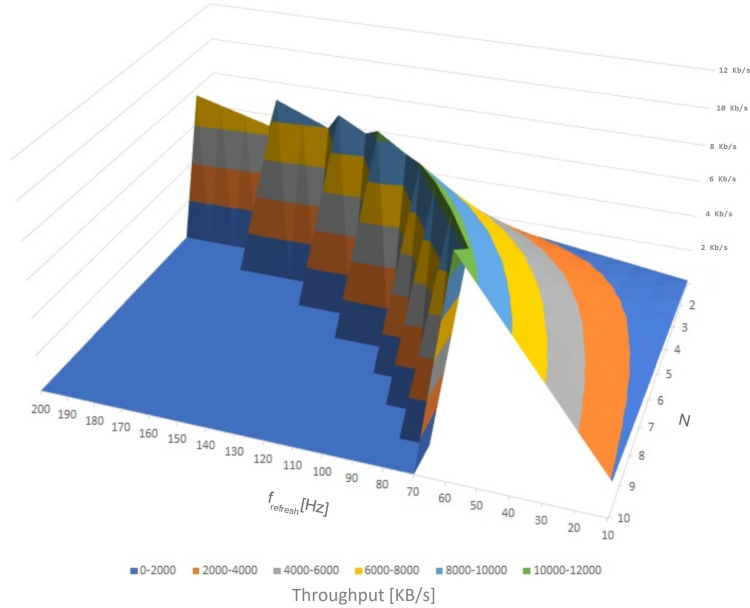


Figure 3.14: Throughput for several pairs $N, f_{refresh}$ with slot equivalent 1.5 ms and Simplex mode configuration.

For clearness, I assign a slot of the same duration to the GW, so that T_{GW} is equivalent to T_{WIS} .

In Fig. 3.14 I have indicated the effective throughput of the pairs $N, f_{refresh}$. For pairs that do not respect equation (3.3), the throughput is 0.

In Table 3.7, I indicate the overall throughput in KB for the possible feasible configurations of the system considering 1.5ms T_{Slot} . For non-feasible configurations, that is that do not respect the equation 3.3, the throughput is 0.

Table 3.7: Throughput T_{Slot} 1.5 ms

N	50 Hz	60 Hz	70 Hz	80 Hz	90 Hz	100 Hz	110 Hz	120 Hz	130 Hz	140 Hz	150 Hz	160 Hz	170 Hz	180 Hz	190 Hz	200 Hz
1	950	1140	1330	1520	1710	1900	2090	2280	2470	2660	2850	3040	3230	3420	3610	3800
2	1900	2280	2660	3040	3420	3800	4180	4560	4940	5320	5700	6080	6460	6840	7220	7600
3	2850	3420	3990	4560	5130	5700	6270	6840	7410	7980	8550	9120	x	x	x	x
4	3800	4560	5320	6080	6840	7600	8360	9120	9880	x	x	x	x	x	x	x
5	4750	5700	6650	7600	8550	9500	10450	x	x	x	x	x	x	x	x	x
6	5700	6840	7980	9120	10260	x	x	x	x	x	x	x	x	x	x	x
7	6650	7980	9310	10640	x	x	x	x	x	x	x	x	x	x	x	x
8	7600	9120	10640	x	x	x	x	x	x	x	x	x	x	x	x	x
9	8550	10260	x	x	x	x	x	x	x	x	x	x	x	x	x	x
10	9500	11400	x	x	x	x	x	x	x	x	x	x	x	x	x	x

Obviously, with a lower T_{Slot} , the overall throughput increases, since the higher frequency and more unit configurations become feasible (3.8).

Table 3.8: Throughput T_{Slot} 1.4 ms

N	50 Hz	60 Hz	70 Hz	80 Hz	90 Hz	100 Hz	110 Hz	120 Hz	130 Hz	140 Hz	150 Hz	160 Hz	170 Hz	180 Hz	190 Hz	200 Hz
1	950	1140	1330	1520	1710	1900	2090	2280	2470	2660	2850	3040	3230	3420	3610	3800
2	1900	2280	2660	3040	3420	3800	4180	4560	4940	5320	5700	6080	6460	6840	7220	7600
3	2850	3420	3990	4560	5130	5700	6270	6840	7410	7980	8550	9120	9690	x	x	x
4	3800	4560	5320	6080	6840	7600	8360	9120	9880	10640	x	x	x	x	x	x
5	4750	5700	6650	7600	8550	9500	10450	x	x	x	x	x	x	x	x	x
6	5700	6840	7980	9120	10260	11400	x	x	x	x	x	x	x	x	x	x
7	6650	7980	9310	10640	x	x	x	x	x	x	x	x	x	x	x	x
8	7600	9120	10640	x	x	x	x	x	x	x	x	x	x	x	x	x
9	8550	10260	11970	x	x	x	x	x	x	x	x	x	x	x	x	x
10	9500	11400	x	x	x	x	x	x	x	x	x	x	x	x	x	x

Considering a network of 10 WIS sampled at 60 Hz, the maximum throughput reaches 11.40 KB/s. Moreover, with a single unit, the 200 Hz sampling is achieved.

As shown in 3.15, the maximum operating frequency, for the fixed number of WIS devices, also depends on the operating mode.

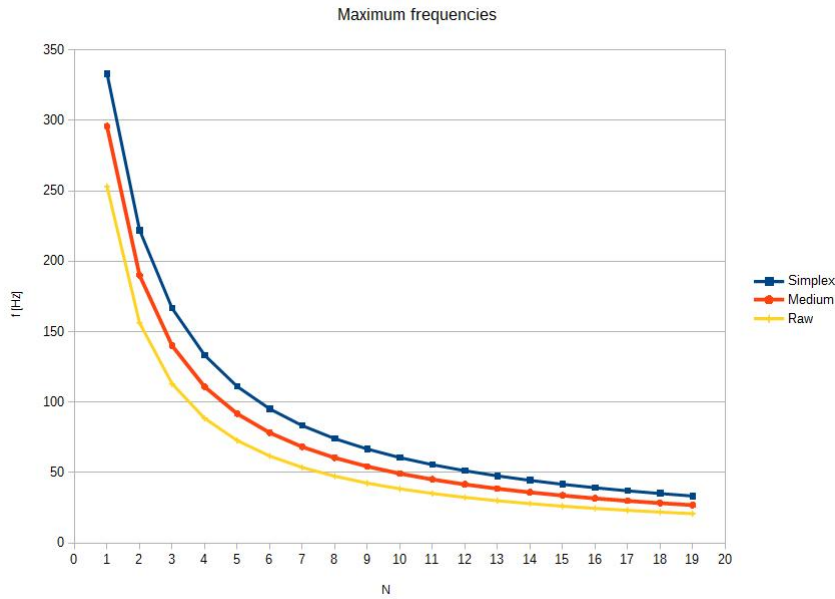


Figure 3.15: The maximum operating frequency according to the operating mode: the payload is 19 B for Simplex, 25 B for Medium, and 49 B for Raw.

3.7.2 Packet Loss

In a TDMA network, it is imperative to keep slot synchronized to avoid overlapping that would deteriorate packets and increase packet loss. In this section, I prove that the constraints are respected through an analysis of network packet loss. The parameter N , variable from 1 to 20, is related to the body segments and joints to monitor, e.g., for shoulder three sensors are enough. To examine it bilaterally, $N =$ five is required, to monitor also elbows bilaterally $N =$ seven [81]. By increasing the sampling rate, I improve the accuracy of movement reconstruction and avoid losing meaningful information.

For a possible acquisition of a bilateral shoulder, I examined different scenarios for the level of interference. In the testbed scenario, I consider a 100 Hz sampling time, and tests lasted 30 minutes; each experiment has been repeated five times. First of all, I observed the ideal case, a building with moderate WiFi interference (4 networks with a power lower than -50 dBm) without any obstacle between the WIS devices and the GW (Test #1). Later I tried to work in a real case with the WIS units attached to the body (Test #2). Then I inserted a loudspeaker piloted via Bluetooth from a smartphone (Test #3). In Table 3.9, I show the averages results obtained for each WIS device and, in the last row, for the overall network. The worst result is for WIS 2 because it was in a position where the body interfered most. The total packet loss of the system is always less than 2% in all scenarios.

Table 3.9: Packet Loss

	Test #1 P.L.	Test #2 P.L.	Test #3 P.L.
WIS 0	0.10 [%]	0.38 [%]	0.60 [%]
WIS 1	0.10 [%]	0.38 [%]	0.53 [%]
WIS 2	0.20 [%]	0.45 [%]	4.15 [%]
WIS 3	0.50 [%]	0.43 [%]	1.65 [%]
WIS 4	0.60 [%]	0.40 [%]	1.23 [%]
NetWIS	0.28 [%]	0.41 [%]	1.63 [%]

3.7.3 Power Consumption

The two microcontrollers have various modes of operation, which affect their performance. In Table 3.10, the main conditions have been evaluated. The measures were

Table 3.10: Power Consumption

MCUs State	V Battery [V]	I Battery [mA]	LifeTime [h]
VLPR	3.8	7	29
RUN	3.8	40,6	4,5
RUN+TX	4	66.1	3,1

implemented through 1,12 Ω shunt resistor. The capacity of the lithium polymer battery is 290 mAh. In the first row, I have both the micro in Very Low Power Mode @ 4 MHz (VLPR). In the second line, I have the MCUs respectively in Run (RUN) @ 40 MHz for KW and RUN @ 80 MHz for K22. Finally, in the last line, I have a possible condition of use: with the processors in the RUN conditions (line 2), sampling at 100 Hz of the sensors by K22, and relative sending of the acquired data.

The value of 3 hours achieved with a 100 Hz transmission, is sufficient for most sports and for clinical sessions, where the patient cannot be stressed for long times [82, 83, 84].

Chapter 4

NB-IoT vs. LoRaWAN

According to the prediction of Ericsson [85], the wireless transmission systems will need to support more than twenty-five billion connected devices. Indeed, it is supposed that the newest 5G wireless mobile communication will provide the technology to support an all-connected world of humans and objects [19].

Today, both NB-IoT and LoRaWAN are offering long-range and low power consumption with the primary aim of being employed as a wireless solution for IoT. However, to the best of my knowledge, there is no detailed comparison helping to select one of these two networking solutions given a specific application scenario. Although some characteristics of the considered technologies, such as the maximum range or the used bandwidth, are not directly comparable, there is a need for a thorough comparison in terms of QoS, deployment cost, and energy consumption.

The main objective of this chapter is an experimental evaluation with in-field measurements of NB-IoT vs. LoRaWAN for IIoT applications. The comparison between the two protocols is performed in terms of power consumption, energy per bit, battery lifetime, and deployment cost. To have a realistic comparison, I use a WSN designed for Structural Health Monitoring (SHM). SHM allows evaluating the aforementioned challenges that are considered the primary obstacles for LPWAN deployments [31, 28].

I conclude that NB-IoT end-device can reach the estimated 10-year battery life only by accumulating many samples in one single message.

4.1 Related Works

Recent literature on energy efficient [86, 87, 88] communication [87, 88], local area network [89], and LPWAN has been very prolific, proposing novel communication protocols and radio technologies. In the long-range communication domain, the most popular protocols are Sigfox, LoRaWAN, and NB-IoT [28, 31, 90]. Sigfox allows remote transfer between devices and an access point through Ultra-narrow Band modulation, with uplink and payload size constraints. Sigfox is very similar to LoRaWAN in terms of power consumption and range [91]. It is less used in IIoT due to its limited payload size (12B) [41], and for the transmission restriction of 140B/day and 4 bytes/day for uplink and downlink respectively [31]. The LoRaWAN open standard enables large scale deployments through LoRa, a chirp spread spectrum

modulation, with a communication range up to 15km at low power operation. Many scientific works describe and model the energy performance for LoRaWAN [92] and the related scalability issues [87, 39]. Moreover, in [32, 93, 94] authors introduce LoRaWAN end-devices with a battery life up to 10 years in real deployments, a standard spec for industrial devices.

The NB-IoT [45] is a variant of LTE (4G Long Term Evolution) developed to fulfill the IoT requirements in civil and industrial applications: coverage extension, long battery lifetime, backward compatibility and user equipment cost reduction are common objectives [46]. The energy performance of NB-IoT is dependent on a multitude of parameters, related to the country's settings and network operator requirement, that can drastically change the end-device average power consumption. In [95] the authors show the NB-IoT independence between the transport block size and power consumption. In this paper, they vary the payload size between 50 and 100 bits, and the measured power consumption is 716mW on average. The energy used to join the network is 11.1J, with a connection time of 36s. In my experiments, I have confirmed the same independence, which is also compared with the LoRaWAN protocol. Low power and lifetime are crucial for wireless end-devices and sensor nodes in IIoT and other applications, as presented on many previous works [20, 28, 96]. In [95] the authors present the NB-IoT power consumption model and in [28] a LoRaWAN comparison analyzing several factors, such as QoS, latency, network coverage, cost and, scalability. They compare both protocols in various use cases, to ensure that LPWAN technologies can provide efficient connectivity solutions across critical and massive IoT deployment, determining their feasibility for specific applications.

Technical differences between NB-IoT and LoRaWAN are summarized in multiple scenarios, such as smart farming [97], manufacturing automation [98], smart building, and logistics [99]. These studies show that both protocols can cooperate in the IoT market: LoRaWAN will serve as the low-cost and very long-range deployments, with infrequent transmissions and heavy constraints in terms of battery life. In contrast, applications requiring low latency and high quality of service, in addition to an international coverage [100], will make use of NB-IoT. The results, about NB-IoT, in [95] and [28] show 13 years of operability with one transmission (TX) per day and 250 days if a packet is sent every hour in power save mode. These numbers decrease drastically, to 126 and 88 days, respectively, if the extended discontinuous reception is enabled (see Section 2.2.3). Finally, [28] concludes that, despite the cellular companies' tests, the NB-IoT power profile currently leaves open questions on the battery life in real deployments.

The primary goal of these previous works is to guide the designers in the difficult task of evaluating the battery lifetime of smart sensors. This work, with a similar intent of the earlier ones, will investigate on the comparison of the two wireless communication protocols. Despite the previous works, I present accurate in-field experimental measurements of LoRaWAN and NB-IoT at the same conditions.

4.2 Experimental Setup

4.2.1 The SHM sensor node

For the comparison, I use a low power wireless sensor developed to measure the cracks in reinforced concrete structures, such as bridges, dams, or skyscrapers [32]. This sensor has been designed to guarantee a high sensitivity, up to $1\mu\text{m}$, combined with an extended battery lifetime, which must be at least ten years measuring and sending data ten times per day. The critical aspects of a wireless sensor node are the radio budget link, power management, and analog front-end.

The sensor node embeds an STM32F373 microcontroller (MCU), an analog front end, and two radio modules: LoRa and NB-IoT operated in a mutually exclusive fashion. The MCU handles the analog and digital parts through the integrated Sigma-Delta ADC converter and the serial peripheral interface. A smart power supply circuit manages a Li-MnO₂ lithium battery (4.2V - 1000mAh) with 80% of efficiency. I select the SX1276 from Semtech [101] that controls the Lora Physical layer and packet buffering. This component achieves a sensitivity of -148dBm with output power up to 20dBm, enabling a 168dB maximum link budget. The NB-IoT transceiver is the SARA-N211 from U-Blox [102]. It is a commercial product provided in the small LGA form factor (16.0×26.0 mm, 96-pin). The module offers data communication over an extended operating temperature with low power consumption, $3\mu\text{A}$ in deep-sleep, and 220mA in transmission at 23dBm. With a receive sensitivity of -135dBm, it offers a 158dBm of link budget. Finally, the M41T82 from ST Microelectronics, an ultra-low-power real-time clock, wakes up the sensor node only at the scheduled time, and it consumes only $365\text{nA}@3\text{V}$.

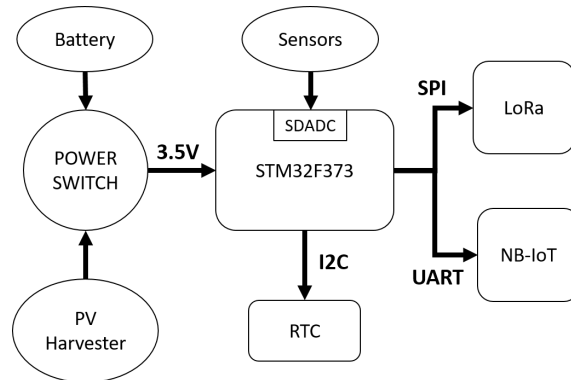


Figure 4.1: Low power wireless crack-meter.

In the active mode, the sensor node draws an average of 23mA (@3V) per second, used to sample, filter, and encrypt the data acquired; the corresponding energy is 70mJ (E_{sensor}). Afterward, the MCU decides which radio protocol must be used depending on the application and user's request. Reducing the wireless communication energy can be very valuable, since the radio transceiver is one of the components with the highest power consumption, as shown in [103]. For each sample, the MCU generates 12 bytes of data, which can be stacked in one buffer or sent immediately

to the application server.

4.2.2 LoRaWAN End-Device Setup

To realistically define an energy profile of the sensor node, I develop a model based on measurements from a real LoRaWAN testbed and previous works [104, 96]. I assume a periodic behavior for each transmission, with a fixed time interval. Therefore I studied the power consumption during one period, which includes the packet generation, the cryptography, the uplink transmission, the RX1 Delay, and, finally, the downlink window used to receive the acknowledge (ACK). Each Datarate (DR) used in this evaluation, from 0 to 5, generates several configurations that impact the LoRa modulation. For example, the Equivalent Bit Rates (EBR) of DR0 and DR5 are respectively 292 and 5469bps (Table 4.1); moreover, the transmission time of air can fluctuate between 225ms to 4s with 100bytes of payload. Such variability impacts the communication range and the power consumption; therefore, smart management of these parameters is crucial to keep the node powered as long as possible. The transmission time takes into account 13 bytes of overhead, LoRaWAN needs to transmit the node's MAC to identify the packet on the server-side correctly. The Coding Rate (CR) and the preamble (N_{pre}) symbols are 4/5, and 8 respectively, and the CRC (Cyclic Redundancy Check) is disabled. Finally, the bandwidth is 125kHz. Under ISO/IEC ISM European regulations, LoRaWAN limits the packet size with a maximum of 51 bytes for DR0 and DR1, and up to 242 for DR5; moreover, since there is a 13 bytes protocol overhead, the payload size is limited to 38 and 229 bytes.

In [104], a study on LoRa SFs assignment is presented. Overestimating the SF may increase the packet error rate (PER) due to low SNR, and an overestimate can significantly decrease the battery lifetime. Applying a PER strategy, where each sensor node assigns the lowest SF for which the PER falls below a fixed threshold, with a 0.01 PER lower limit [104], the SFs are allocated about 43% SF12, 20% SF11, 12% SF10, 8% SF9, 6% SF8, and 11% SF7. Since most of the sensor nodes are in high SF zone, in my work, I consider the maximum packet size of 51 bytes for all the configurations; this allows a queue of three samples, corresponding to three crack measurements in one single packet. In [105] and [92], the authors show the correlation between network traffic and packet loss: they indicate a 10% packet loss for architectures with 1000 nodes, 36% for 5000, 59% for 10000. Following, [104] shows the effect of saturating the available airtime with one gateway and a large number of nodes. They simulate an upstream scenario with a data period of 6000s and 21B of payload. With the proposed SF assignment, the PER increases significantly when the number of devices exceeds 5000. Concerning the environments, a recent study [106] evaluates the packet loss under challenging environments, such as a data center facility and indoor industrial establishments. In these conditions, the packets received with the wrong CRC vary between 0.5% and 6%. Hence in my SHM testbed, the PER is not negligible and must be taken into account to estimate the average energy consumption. The SX1276 [107], with the power amplifier enabled, generates a current consumption of 87mA@17dBm in TX and 11.5mA in RX at 3V; moreover, the overall energy per packet is highly correlated with the packet time of air. The sensor node uses the Class A operating mode.

4.2.3 NB-IoT End-Device Setup

U-Blox makes available only uplink, downlink, and sleep power details, which are respectively 220mA (averaged current over 2 seconds @ 23 dBm), 46mA, and $6\mu\text{A}$. For this reason, it is difficult to estimate the energy used by the transceiver during the entire sensor node life since the NB-IoT standard has a multitude of parameters, such as the eDRX and PSM timers, the transmission power and the number of repetitions requested by the network. It is not trivial to estimate the EPB from the power consumption model without measurements in real deployment [95]. Thus, I combine a model based on measurements from a real NB-IoT testbed, and previous works [28, 95] to precisely derive the NB-IoT energy profile.

I tested the SHM sensor node, varying the payload and the RSSI that influences the power consumption of the module. The testbed is deployed in Switzerland, Europe, where the ISM (Industrial Scientific Medical) band is at 863-870MHz. Precisely, I define the -80dBm average RSSI as Good (G), -110dBm average RSSI as Medium (M), and finally, -130 dBm average RSSI as Bad (B).

4.3 Experimental Results

This section presents the experimental evaluation of the SX1276 and SARA-N211 modules in the above mentioned experimental setup. In particular, I focus on the energy performance of the SHM sensor node with multiple payload sizes and coverage conditions to determine the battery lifetime. The sensor node periodically transmits an uplink message, which can include a single sample or multiple acquisitions queued in one packet.

4.3.1 LoRaWAN End-Device Analysis

Table 4.1 presents the measured payload Energy Per Bit (EPB) with different DRs and sizes, considering the power used in TX, in RX and the energy used by the MCU to encrypt and decrypt the data: EPB1 refers to 1 sample (12B), EPB2 contains 2 (24B) and EPB3 3 (36B). Moreover, Table 4.1 shows that the DR0 uses $22\times$ more energy in comparison with DR5. As expected, the EPB does not scale linearly with

Table 4.1: LoRaWAN EPB & EPP

DR	SF	EBR [bps]	EPB 1 [mJ]	EPB 2 [mJ]	EPB 3 [mJ]	Packet 1 [mJ]	Packet 2 [mJ]	Packet 3 [mJ]
DR0	12	293	6.69	5.31	4.00	641.28	1017.60	1152.01
DR2	10	977	1.68	1.30	1.01	161.28	249.59	290.88
DR5	7	5469	0.30	0.23	0.16	28.32	43.2	46.08

the payload due to the high ratio between preamble and payload size. For example, with 12 bytes and DR5, the preamble length is the 35% of the overall time of air, and with 100 bytes, it is only the 6%. This result states that buffering the samples in one packet increases the transmission energy performance.

To carefully model the sensor node behavior, I measured the energy consumption for the first connection and authentication with the LoRaWAN server; this procedure exchanges the cryptography keys and establishes a secure connection between devices. The values measured for DR0,2 and 5 are respectively 581.29mJ, 172.25mJ, and 62.03mJ. In the last three columns, Table 4.1 presents the overall Energy Per Packet (EPP) for a LoRaWAN transmission in the SHM application with different DRs and queue lengths: Packet 1 includes only one crack measurement (12 bytes of payload) whereas Packet 3 is composed of three. EPP values in Table 4.1, and the equivalent T_{Packet} in Eq. 4.1, take into account the uplink packet (T_{tx} - Eq. 4.2) formed by the payload (PL), preamble and 13 bytes of LoRaWAN overhead, the waiting period (T_{rx1}) between the uplink and downlink windows and lastly, the receive period used to detect the ACK (T_{rxw}). Equation 4.2 highlights that the transmission time of a packet is a function of SF and BW.

$$T_{Packet} = T_{tx} + T_{rx1} + T_{rxw} \quad (4.1)$$

$$T_{tx} = \frac{2^{SF}}{BW} \cdot (N_{pre} + 4.25 + N_{PHY}) \quad (4.2)$$

$$N_{PHY} = 8 + \max \left[\text{ceil} \left[\frac{28 + 8 \cdot PL - 4 \cdot SF}{4 \cdot SF} \right] \cdot (CR + 4), 0 \right] \quad (4.3)$$

T_{tx} expresses the time in seconds required to transmit both the preamble and the payload; the latter is composed of the number of symbols calculated in Eq. 4.3. The EPB presented in Table 4.1 provides the energy for a single bit in PL, hiding the LoRa modulation behavior.

4.3.2 NB-IoT End-Device Analysis

This section focuses on the NB-IoT energy performance of the sensor node in the same deployment conditions as the previous subsection. Table 4.2 shows the measurements of energy per packet and T_{active} with 10,50,100 and 400 bytes of payload, depending on the 3 defined coverage levels. Column E_{mean} is a result of 50 successive measurements with the same RSSI condition to model the average energy performance for each one of the presented 12 tests. The RSSI is the most relevant element to estimate the battery lifetime. Dividing the values in Table 4.2 for coverage conditions, the absence of correlations between energy and payload size (Table 4.2 - N bytes) can be appreciated. Indeed, between (a) and (d) the T_{active} and E_{mean} differences are respectively 2% and 10% sending $40 \times$ more bytes. Similar behaviour can be detected in B coverage, between tests (i) and (n), where the T_{active} ranges between 37.2s in (m) and 46.6s in (i); the E_{mean} is included in a 25% of variability. These measurements have been carried out with the Swisscom network provider, which releases the default 3 minutes period for T3324, whereas the T3412 can be set up to 310 hours, avoiding TAU signaling between successive uplinks. The T3324 energy consumption must be added for each transmission because the SARA-N211 module is awake in listening mode. The overall value for 3 minutes timer is 844mJ, equal for each coverage condition.

Table 4.2: NB-IoT Energy Characterization

ID	C	N bytes	$T_{act.}$ [s]	I_{max} [mA]	E_{mean} [mJ]	E_{max} [mJ]	E_{min} [mJ]	RSSI [dBm]
<i>a</i>	G	10	11.9	138	2063	3007	517	-83
<i>b</i>	G	50	11.9	146	1858	3111	486	-81
<i>c</i>	G	100	12.0	135	1856	3240	499	-75
<i>d</i>	G	400	12.2	138	2067	3232	550	-75
<i>e</i>	M	10	13.7	245	2677	4549	1847	-112
<i>f</i>	M	50	12.8	232	2453	4078	1890	-109
<i>g</i>	M	100	12.6	219	2379	4150	1903	-110
<i>h</i>	M	400	12.8	225	2386	3786	1972	-107
<i>i</i>	B	10	46.6	151	9047	17072	5453	-130
<i>l</i>	B	50	41.1	175	7641	16298	5579	-136
<i>m</i>	B	100	37.2	169	6818	13264	5200	-135
<i>n</i>	B	400	40.5	185	7552	17845	5745	-134

The maximum energy measured in G condition (test (*a*)) is $6\times$ higher compared to minimum, and the (*n*) test maximum energy is $37\times$ the test (*b*). Studying the Table 4.2 and the Figure 4.2, I detect a significant increase of the variance in B than M and G coverage. These results disclose the high power consumption variability of the NB-IoT, which is not under the direct control of the user. Indeed, each network provider manages differently the network parameters, such as the number of repetitions, the transmission power, TAU, and eDRX timers. For future designs, Table 4.2 - I_{max} is a useful detail for the power management calculations.

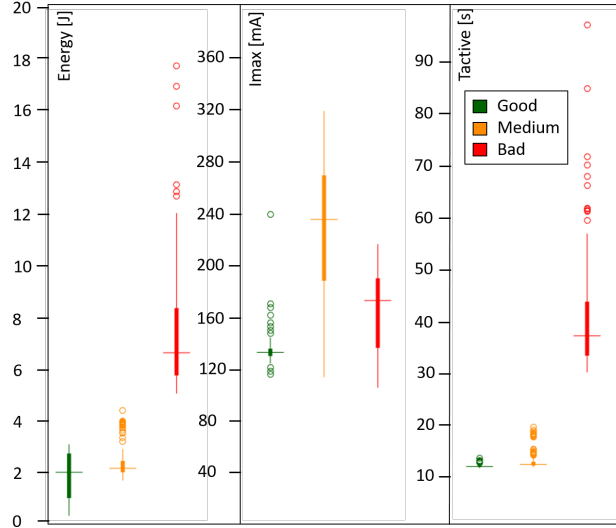


Figure 4.2: NB-IoT characterization with median, 25th, and 75th percentiles. Good (G) in green with an average RSSI of -80dBm, Medium (M) in orange with an average RSSI of -110dBm and, Red (R) with an average RSSI of -130 dBm.

The good coverage group, in green, has an average RSSI of -80dBm; this generates a mean T_{active} of 12s; with these parameters, the average energy for each packet is 1982mJ. In the M group, the T_{active} slightly increases, with a mean of 13s, but the resulting energy 2474mJ grows of about 25% in comparison with good coverage; indeed, the maximum current is 100mA higher. This behavior means that the NB-IoT cell increases the output power before raising the number of retransmissions. In analogy with LoRa, the NB-IoT's T_{active} is highly correlated with the communication latency that for the latter reaches up to 46s in worst cases (Table 4.2). Tests $(i),(l),(m),(n)$ are close to the maximum sensitivity of the module, the resulting energy, and T_{active} grow heavily: the average time is 41s with a maximum of 17845mJ and, a medium of 7765mJ.

Figure 4.2 presents the statistical analysis of the Energy, I_{max} and T_{active} features showing the median, 25th, and 75th percentiles of all the data acquired (600 samples). The energy grows with respect to the received RSSI decrease, which is the result of the T_{active} and I_{max} combination depending on the coverage strength and the network request. Indeed, the NB-IoT protocol raises the output power in TX before increasing the number of retransmissions, and the correlated T_{active} . The packet time difference between G and M is negligible, but B's T_{active} is at least $3\times$ compared to G. Furthermore, in M the output power correlated with the I_{max} is $2\times$ and $1.3\times$ compared with G and B respectively, but the T_{active} is still comparable with B.

To carefully model the sensor node behavior, I checked the energy used for the first connection and authentication with the NB-IoT cell; this procedure subscribes to the sensor node on the network. The values measured for G, M, and B are respectively 15843, 17182, and 19124mJ, with an average connection time of 80 s. NB-IoT enables a packet length up to 1600 bytes [108], but the used module (with firmware version: 0.6.57, A07) is limited. Consequently, the queue is restricted to 33 samples, each consisting of 12 bytes. In Table 4.3, I present payload EPB with different coverages and sizes: EPB 1: 12 bytes of payload (1 sensor samples); EPB 2: 24 bytes of payload (2 sensor samples); EPB 3: 36 bytes of payload (3 sensor samples); EPB 8: 96 bytes of payload (8 sensor samples); EPB 33: 396 bytes of payload (33 sensor samples).

Table 4.3: NB-IoT EPB

C	EPB 1 [mJ]	EPB 2 [mJ]	EPB 3 [mJ]	EPB 8 [mJ]	EPB 33 [mJ]
G	29.4	14.8	9.8	3.6	0.9
M	34.5	17.2	11.5	4.2	1.0
B	89.6	44.9	29.9	11.2	2.7

The EPB in Table 4.3 takes into account the uplink energy used in T_{active} and T3324 periods: it is clear that the equivalent EPB decreases increasing the queue size, as presented in the recent literature [95].

Compared to LoRaWAN, sending one sample per packet with NB-IoT reduces the battery life drastically, as I will present in the following subsection. Moreover, the T_{active} does not depend from payload length but is strictly correlated with the

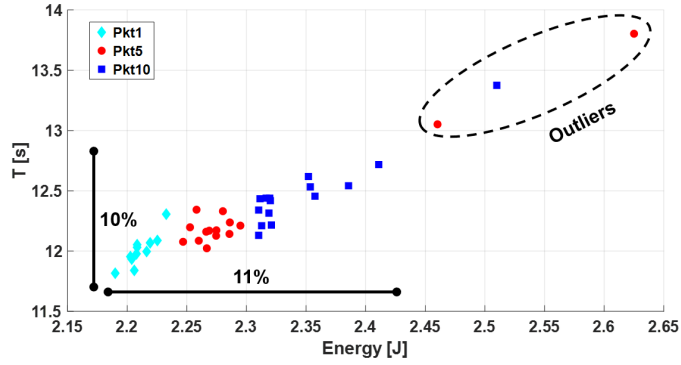


Figure 4.3: Differences between single and multiple packet transmissions in a single connection.

coverage condition, i.e., the average RSSI; in fact, the NB-IoT protocol increases the number of retransmissions from 32 to 2048 when the RSSI is low. As expected, power consumption is independent of the uplink and downlink data rate [95]. I measured that the energy consumption between packets in static working conditions varies respect to network parameters requested by the operator: the output power, the number of retransmissions, and the T_{active} can be modified between successive uplinks, and are not under the direct control of the U-Blox module. To prove the NB-IoT inefficiency for sporadic and tiny transfers, I performed the measures presented in Figure 4.3. Taking as reference the Test (d), I evaluate the T_{active} and the E_{mean} sending one to ten successive packets with 400 bytes of payload in G coverage. In contrast to LoRaWAN, the energy does not grow linearly with the number of uplinks in a single connection (Figure 2.7 - DATA), but it only increases of 11% sending ten times more bytes. The outliers values showed in Figure 4.3 may be motivated by the fact that the NB IoT network sometimes changes parameters asynchronously. In this case, the higher energy measured for the procedure may have been erroneously considered in the transmission. In the Pkt10 condition, the EPB is about 0.1mJ, 9x less than the EPB 33 presented in Table 4.3. However, a buffer of 330 samples could generate an excessive latency for many applications; hence, in this chapter, I will compare the EPB considering only one transfer for each connection, as well as commonly used in a deployment where sporadic transmissions are required. Finally, the expected E_{mean}^* generated in a single connection where multiple packets are transferred, is presented in Eq. 4.4. The C variable points at the coverage condition energy in Table 4.2 - E_{mean} and N_{pkt} is the number of packets transmitted together.

$$E_{mean}^*(C) = E_{mean}(C) \cdot (1 + N_{pkt} \cdot 0.01) \quad (4.4)$$

4.3.3 Battery life and comparisons

This subsection focuses on the estimation of the battery life in the SHM application scenario based on the above-presented power measurements. One of the most challenging features of SHM applications is to achieve a lifetime of 10 years. In my

evaluation, I assume each node equipped with a 1000 mAh lithium battery @3V, which is a widely used type of battery for SHM nodes [32]. It is also a widely used battery capacity value for evaluations of other WSN applications [109, 110, 111]. Thus, the energy consumption for each sensor's sampling is constrained, and its usage is regulated by the energy per packet and the queue length. For the estimation, I consider the energy used for the initial connections ($E_{connection}$) calculated in previous sections with 10 samples per day (N_{tx}) to fulfill the plots in Figure 4.4. In particular, based on previous considerations, the average packet loss changes considerably depending on every single deployment, varying between 0% to 60% due to crowded radio channels or electromagnetic noisy environments. Hence it is misleading to provide a single result for each configuration. I consider the packet loss probability for energy estimation in the LoRaWAN case study and, the Figure 4.4 takes into consideration the effective communication variability, providing a lower and upper bound between 0-60% ($P_{PktLoss}$). For a conservative parameter, it is important to consider the integer bar to estimate the average sensor working span depending on the queue and DR configurations. Eq. 4.5 and Eq. 4.6 show the formulas used to calculate the data in Figure 4.4 for LoRaWAN and NB-IoT respectively. T_{LoRa} and T_{NB-IoT} provide the times in days, E_{SLEEP} is the sleep energy calculated with a 365nA current. Lastly, C and Q select the coverage and queue configurations from Table 4.1 and Table 4.3.

$$\begin{cases} T_{LoRa} = \frac{(DCDC_{eff} \cdot E_{batt}) - E_{connection}(C)}{[E_{LoRa} + E_{sensor}] \cdot \frac{N_{tx}}{Q} + E_{SLEEP}} \cdot 86400s \\ E_{LoRa} = \left(12 \cdot Q \cdot 8 \cdot EPB(C, Q) \cdot \frac{1}{1 - P_{PktLoss}} \right) \end{cases} \quad (4.5)$$

$$T_{NB-IoT} = \frac{(DCDC_{eff} \cdot E_{batt}) - E_{connection}(C)}{[E_{mean}^*(C) + E_{sensor}] \cdot \frac{N_{tx}}{Q} + E_{SLEEP}} \cdot 86400s \quad (4.6)$$

The resulting lifetime is less than ten years with Packets 1-8 for both protocols in DR0/Bad coverage (Figure 4.4), but it is interesting to notice that with Packets 1-3 LoRaWAN reaches this threshold in DR2 and DR5. NB-IoT allows this duration only with Packet 33, in all coverage conditions; on the other side, LoRaWAN reaches the target from DR2 without queuing. If the application requires a transmission for each sample, the expected lifetime is respectively 4.5 months and 3.5 years for NB-IoT and LoRaWAN in the worst case. As shown in Figure 4.4, with equal coverage, NB-IoT EPB is an order of magnitude higher than that measured with LoRaWAN.

The LoRaWAN EPB decreases more if coverage improves compared to the use of buffering techniques, as opposed to NB-IoT, where the decrease is similar. Finally, the only cases where EPB is advantageous for NB-IoT is when the coverage is at least DR2/M and the message sent contains 33 samples (Packet 33).

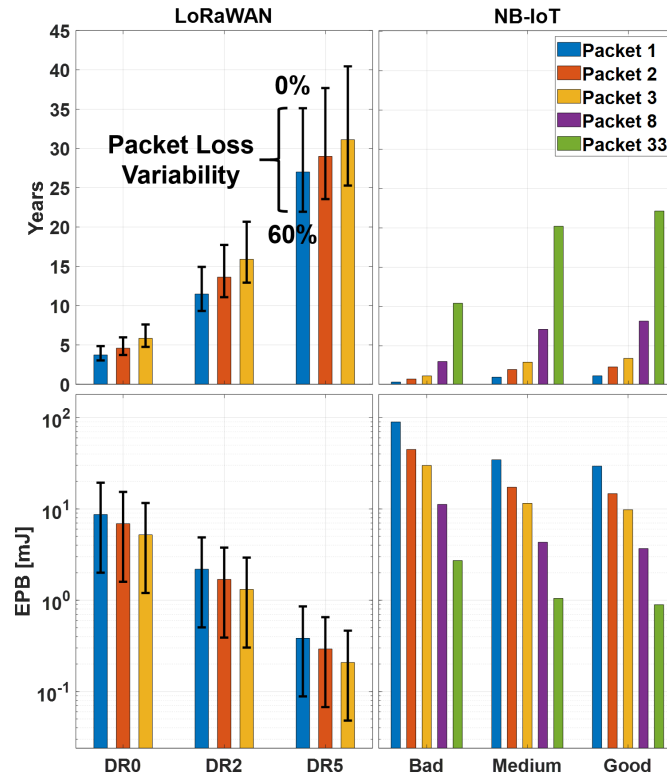


Figure 4.4: Expected battery lifetime and EPB with LoRaWAN and NB-IoT. End-device coverage is divided into: DR0/Bad with an average RSSI of -130 dBm, DR2/Medium with an average RSSI of -110dBm and, DR5/Good with an average RSSI of -80dBm.

Chapter 5

Long-Range Deployments Guidelines

Wireless communication energy consumption is the principal issue in IIoT applications. Nevertheless, many factors should be considered, including the QoS, the cost, and the coverage. In this chapter, I provide guidelines for the selection and the deployment of the most suitable technology, based on the collected measurements of the previous chapter and the current knowledge of the two tested solutions.

5.1 Quality of Service and Coverage

The QoS benefits of using a licensed bandwidth technology have already been introduced in the Chapter 2.3. This work highlights that LoRaWAN works on unlicensed ISM channels with an asynchronous protocol, and, in crowded channels and industrial environments, the packet loss cannot be considered as a negligible factor, given that it can decrease the expected battery lifetime up to 37%. On the other hand, NB-IoT offers an optimal QoS, with guaranteed data delivery, working on a licensed spectrum, and an LTE-based synchronous protocol. However, its communication latency is not optimal. Indeed, the maximum LoRaWAN packet time, which corresponds to the transfer delay, is 2630ms with DR0. It is 17x lower than the NB-IoT's T_{active} in B coverage (Table 4.2 - *i*).

Moreover, for national scale coverage applications, for example, in the monitoring of transportable goods to determine the pallet locations on highways or railroads, the use of NB-IoT is the only solution due to the infrastructure already provided by the network operators. To cover limited areas or remote areas where network operators do not offer good coverage, LoRaWAN devices with dedicated support can instead be more efficient.

5.2 Cost and Time To Market

Cost and time to market (TTM) are two fundamental parameters when a company wants to develop a business with a technology based on an LPWAN. Different parameters must be examined for the implementation costs. A generic NB-IoT module can exceed 20€ compared to 3-5€ of a LoRa transceiver [28]. Moreover, it is important to consider the cost related to traffic generated by each device (500MB of traffic are

priced today at 10€. This amount of data is more than enough for the entire sensor life in a typical monitoring application. On the other hand, a LoRaWAN network must have at least one access point (300€/gateway) and the server (1000€/base station). In the considered SHM application, the system generates 120 bytes daily, allowing more than 100 years of hypothetical operation with a single subscription.

In summary, Eq. 5.1 quantifies the deployment cost of the two technologies.

$$\begin{cases} Cost_{NB-IoT} = (Cost_{module} + Cost_{SIM}) \cdot N \\ Cost_{LoRa} = Cost_{module} \cdot N + Cost_{Gateway} + Cost_{Server} \end{cases} \quad (5.1)$$

Considering that Mobile Network Operators (MNOs) also take care of the maintenance of the infrastructure, in the LoRaWAN terms $Cost_{Gateway}$ and $Cost_{Server}$ must be taken into account these added costs.

Whenever the number (N) of sensor nodes is a few tens, the NB-IoT is more affordable due to the high installation cost of LoRaWAN gateway and server, as shown by Eq. 5.1, enabling quicker TTM in regions where the LoRaWAN is not deployed yet. On the other hand, LoRaWAN is today more affordable for large-scale deployments, due to the higher cost of NB-IoT modules.

When the TTM is a concern, NB-IoT has an advantage because of the plug-and-play service offered by network operators.

5.3 Security

Finally, ensuring security in IoT deployments is challenging. NB-IoT uses two security levels inherited from LTE, access stratum (AS) and non-access stratum (NAS) security. AS security is established between the device and the base station (BS), whereas NAS security is constituted by the device and the mobility management entity (MME). The 3GPP defines four ciphering algorithms, denoted as EPS encryption algorithms (EEAs), and four integrity algorithms, known as EPS integrity algorithm (EIA) applied for the communication between the devices and, respectively, the BS or MME. The EEA0 algorithm shall be implemented such that it has the same effect as if it generates an encryption key of all zeroes; the 128-EEA1 algorithm is based on SNOW 3G; the 128-EEA2 is based on 128-bit AES in CTR mode, the 128-EEA3 is based on ZUC. For more details, see Appendix B of [112]. These algorithms are chosen based on the security skills of the device.

The LoRaWAN security mechanisms rely on the AES cryptographic algorithm. Mutual authentication is established between an end-device and the LoRaWAN server as part of the network join procedure. It ensures that only authorized devices can join the network. LoRaWAN MAC is origin authenticated, integrity protected, replay protected, and encrypted. Moreover, it implements end-to-end encryption for application payloads exchanged between the devices and the servers. Each device is programmed with two AES Key: 128-bit AppKey and a 64-bit globally unique identifier.

[112]

Chapter 6

Conclusion

The Internet of Things is a concept, which is currently under progress. The idea to connect everything and anything and anytime is appealing. The first part of this study performed in this work explores the diverse characteristics of several MAC layer protocols used in the IoT world. The aspects addressed here are mainly related to physical and MAC layers bringing a comparative panorama to the range coverage, data rates, and energy efficiency aspects. This starting point was preparatory to the development of the Capture motion system designed in the company during the first part of the Ph.D. A novel hardware-software solution for the body sensor network has been presented. Multiple sensors node and a gateway compose the system, which maximizes the throughput by a robust communication protocol and increases the scalability. Experimental results in the field show the performance achieved. The developed system offers higher performance as data throughput for configurations below ten nodes, compared to the Xsens MVN Awinda sensors that transmit 60 Hz frequency [62]. In terms of weight and size, the proposed system is equivalent. Each network can be calibrated at a different frequency, making the system more flexible, depending on the motion capture application.

The second contribution of this thesis was to evaluate two technologies in the Long Range world of communications. From the business point of view, knowledge has been acquired that can orient itself among the various stacks available based not only on the data reported but also on experimental data that are not easy to find in the literature. This work evaluates LoRaWAN and NB-IoT as wireless communication technologies for industrial application scenarios that require to transfer a few bytes per day. The evaluation is based on experimental results obtained in-field expecting a sensor node for crack measurements in civil structures. We evaluate both technologies with experimental results in different coverage conditions, intending to assess the energy consumption, the estimated battery lifetime, and the packet loss. My assessment shows that LoRaWAN outperforms NB-IoT in terms of energy consumption. In an application where stacked measurements are not allowed, the LoRaWAN protocol increases the battery life up to $10\times$ against NB-IoT. For Packet 3 scenario (36 Bytes payload), DR2 / M Coverage, NB-IoT EPB is $10\times$ higher compared to LoRaWAN. However, NB-IoT is adequate for applications where information can be buffered on the node because the energy for each transmission is independent of the payload size. For example, in Packet 33 scenario (396 Bytes pay-

load), DR2 / M Coverage, NB-IoT EPB is $11\times$ lower compared to LoRaWAN, due to its more messages sent. Moreover, I verify that T_{active} in the NB-IoT is heavily dependent on network coverage, as it grows up to $3\times$ times passing from a "Good" (average RSSI of -80dBm) coverage to a "Bad" one (average RSSI of -130dBm). On the other hand, NB-IoT offers the highest QoS, which guarantees data delivery. This feature makes it a potential replacement to LoRaWAN in all the applications where energy is provided by the electricity grid or when communication reliability is a crucial factor.

Bibliography

- [1] Kevin Ashton et al. That ‘internet of things’ thing. *RFID journal*, 22(7):97–114, 2009.
- [2] In Lee and Kyoochun Lee. The internet of things (iot): Applications, investments, and challenges for enterprises. *Business Horizons*, 58(4):431–440, 2015.
- [3] Andrew Whitmore, Anurag Agarwal, and Li Da Xu. The internet of things—a survey of topics and trends. *Information Systems Frontiers*, 17(2):261–274, 2015.
- [4] Dhananjay Singh, Gaurav Tripathi, and Antonio J Jara. A survey of internet-of-things: Future vision, architecture, challenges and services. In *2014 IEEE world forum on Internet of Things (WF-IoT)*, pages 287–292. IEEE, 2014.
- [5] H Arasteh, V Hosseinnezhad, V Loia, A Tommasetti, O Troisi, M Shafie-Khah, and P Siano. Iot-based smart cities: a survey. In *2016 IEEE 16th International Conference on Environment and Electrical Engineering (EEEIC)*, pages 1–6. IEEE, 2016.
- [6] Partha Pratim Ray. A survey on internet of things architectures. *Journal of King Saud University-Computer and Information Sciences*, 30(3):291–319, 2018.
- [7] How the internet of things will transform consumerism, enterprises, and governments over the next five years. [online] www.businessinsider.com/7-27-2018-iot-forecast-book-2018-7?ir=t.
- [8] Ala Al-Fuqaha, Mohsen Guizani, Mehdi Mohammadi, Mohammed Aledhari, and Moussa Ayyash. Internet of things: A survey on enabling technologies, protocols, and applications. *IEEE communications surveys & tutorials*, 17(4):2347–2376, 2015.
- [9] Luiz Oliveira, Joel JPC Rodrigues, Sergei A Kozlov, Ricardo AL Rabêlo, and Victor Hugo C de Albuquerque. Mac layer protocols for internet of things: A survey. *Future Internet*, 11(1):16, 2019.
- [10] Prosanta Gope and Tzonelih Hwang. Bsn-care: A secure iot-based modern healthcare system using body sensor network. *IEEE Sensors Journal*, 16(5):1368–1376, 2015.

- [11] Xsens, <https://www.xsens.com>.
- [12] Shimmer sensing website, <http://www.shimmersensing.com>.
- [13] E. Farella, A. Pieracci, D. Brunelli, L. Benini, B. Ricc3, and A. Acquaviva. Design and implementation of wimoca node for a body area wireless sensor network. In *2005 Systems Communications (ICW'05, ICHSN'05, ICMCS'05, SENET'05)*, volume 2005, pages 342–347, Aug 2005.
- [14] Taiyang Wu, Fan Wu, Jean-Michel Redout3, and Mehmet Rasit Yuce. An autonomous wireless body area network implementation towards iot connected healthcare applications. *Ieee Access*, 5:11413–11422, 2017.
- [15] Hsueh-Chun Lin, Shu-Yin Chiang, Kai Lee, and Yao-Chiang Kan. An activity recognition model using inertial sensor nodes in a wireless sensor network for frozen shoulder rehabilitation exercises. *Sensors*, 15(1):2181–2204, 2015.
- [16] Yushuang Tian, Xiaoli Meng, Dapeng Tao, Dongquan Liu, and Chen Feng. Upper limb motion tracking with the integration of imu and kinect. *Neuro-computing*, 159:207–218, 2015.
- [17] Sumit Majumder, Tapas Mondal, and M Deen. Wearable sensors for remote health monitoring. *Sensors*, 17(1):130, 2017.
- [18] Marco Muraccini, Anna Lisa Mangia, Maurizio Lannocca, and Angelo Cappello. Magnetometer calibration and field mapping through thin plate splines. *Sensors*, 19(2):280, 2019.
- [19] Fei Tong, Yuyi Sun, and Shibo He. On positioning performance for the narrow-band internet of things: How participating enbs impact? *IEEE Transactions on Industrial Informatics*, 15(1):423–433, 2019.
- [20] Silia Maksuti, Ani Bicaku, Markus Tauber, Silke Palkovits-Rauter, Sarah Haas, and Jerker Delsing. Towards flexible and secure end-to-end communication in industry 4.0. In *2017 IEEE 15th International Conference on Industrial Informatics (INDIN)*, pages 883–888. IEEE, 2017.
- [21] Ling Lyu, Cailian Chen, Shanying Zhu, and Xinping Guan. 5g enabled code-sign of energy-efficient transmission and estimation for industrial iot systems. *IEEE Transactions on Industrial Informatics*, 14(6):2690–2704, 2018.
- [22] Nataša Banović-Ćurguz, Dijana Ilišević, and Djuradj Budimir. Towards digital transformation with 5g technology. *International Journal of Electrical Engineering and Computing*, 2(2):101–110, 2018.
- [23] Marina Indri, Antoni Grau, and Michael Ruderman. Guest editorial special section on recent trends and developments in industry 4.0 motivated robotic solutions. *IEEE Transactions on Industrial Informatics*, 14(4):1677–1680, 2018.
- [24] Lora. [online]. available:www.lora-alliance.org/.

- [25] Sigfox. [online]. available: <http://www.sigfox.com>.
- [26] 3GPP. [3gpp tr 45.820 v13.1.0. “cellular system support for ultra-low complexity and low throughput internet of things (ciot), November 2015.
- [27] Pilar Andres-Maldonado, Pablo Ameigeiras, Jonathan Prados-Garzon, Jorge Navarro-Ortiz, and Juan M Lopez-Soler. Narrowband iot data transmission procedures for massive machine-type communications. *IEEE Network*, 31(6):8–15, 2017.
- [28] Kais Mekki, Eddy Bajic, Frederic Chaxel, and Fernand Meyer. A comparative study of lpwan technologies for large-scale iot deployment. *ICT Express*, 2018.
- [29] Rashmi Sharan Sinha, Yiqiao Wei, and Seung-Hoon Hwang. A survey on lpwa technology: Lora and nb-iot. *Ict Express*, 3(1):14–21, 2017.
- [30] Martin C Bor, John Vidler, and Utz Roedig. Lora for the internet of things. In *EWSN*, volume 16, pages 361–366, 2016.
- [31] Godfrey Anuga Akpakwu, Bruno J Silva, Gerhard P Hancke, and Adnan M Abu-Mahfouz. A survey on 5g networks for the internet of things: Communication technologies and challenges. *IEEE Access*, 6:3619–3647, 2018.
- [32] Tommaso Polonelli, Davide Brunelli, Marco Guermandi, and Luca Benini. An accurate low-cost crackmeter with lorawan communication and energy harvesting capability. In *2018 IEEE 23rd International Conference on Emerging Technologies and Factory Automation (ETFA)*, volume 1, pages 671–676. IEEE, 2018.
- [33] Alberto Girolami, Federica Zonzini, Luca De Marchi, Davide Brunelli, and Luca Benini. Modal analysis of structures with low-cost embedded systems. In *Circuits and Systems (ISCAS), 2018 IEEE International Symposium on*, pages 1–4. IEEE, 2018.
- [34] José Vera-Perez, David Todoli-Ferrandis, Víctor Sempere-Payá, Rubén Ponce-Tortajada, Gabriel Mujica, and Jorge Portilla. Safety and security oriented design for reliable industrial iot applications based on wsns. In *2019 24th IEEE International Conference on Emerging Technologies and Factory Automation (ETFA)*, pages 1774–1781. IEEE, 2019.
- [35] IEEE Computer Society LAN MAN Standards Committee et al. Wireless lan medium access control (mac) and physical layer (phy) specifications. *ANSI/IEEE Std. 802.11-1999*, 1999.
- [36] Jan Magne Tjensvold. Comparison of the ieee 802.11, 802.15. 1, 802.15. 4 and 802.15. 6 wireless standards. In *IEEE: September*, volume 18, 2007.
- [37] IEEE Computer Society. Ieee standards ieee 802.15.4-part 15.4—wireless mac and phy specifications for low-rate wireless personal area networks—lr-wpans. 2003.

- [38] N Sornin, M Luis, T Eirich, T Kramp, and O Hersent. Lorawan specification. *LoRa alliance*, 2015.
- [39] Tommaso Polonelli, Davide Brunelli, Achille Marzocchi, and Luca Benini. Slotted aloha on lorawan-design, analysis, and deployment. *Sensors*, 19(4):838, 2019.
- [40] Phui San Cheong, Johan Bergs, Chris Hawinkel, and Jeroen Famaey. Comparison of lorawan classes and their power consumption. In *Communications and Vehicular Technology (SCVT), 2017 IEEE Symposium on*, pages 1–6. IEEE, 2017.
- [41] Kais Mekki, Eddy Bajic, Frederic Chaxel, and Fernand Meyer. Overview of cellular lpwan technologies for iot deployment: Sigfox, lorawan, and nb-iot. In *2018 IEEE International Conference on Pervasive Computing and Communications Workshops (PerCom Workshops)*, pages 197–202. IEEE, 2018.
- [42] Guillaume Ferré and Eric Simon. An introduction to sigfox and lora phy and mac layers. 2018.
- [43] Claire Goursaud and Jean-Marie Gorce. Dedicated networks for iot: Phy/mac state of the art and challenges. 2015.
- [44] Marco Centenaro, Lorenzo Vangelista, Andrea Zanella, and Michele Zorzi. Long-range communications in unlicensed bands: The rising stars in the iot and smart city scenarios. *IEEE Wireless Communications*, 23(5):60–67, 2016.
- [45] Qualcomm. Qualcomm, incorporated, narrowband iot (nb-iot), rp-151621, 3gpp tsg ran meeting #69, sept. 2015. [online]., 2015.
- [46] Y-P Eric Wang, Xingqin Lin, Ansuman Adhikary, Asbjorn Grovlen, Yutao Sui, Yufei Blankenship, Johan Bergman, and Hazhir S Razaghi. A primer on 3gpp narrowband internet of things. *IEEE Communications Magazine*, 55(3):117–123, 2017.
- [47] Ansuman Adhikary, Xingqin Lin, and Y-P Eric Wang. Performance evaluation of nb-iot coverage. In *Vehicular Technology Conference (VTC-Fall), 2016 IEEE 84th*, pages 1–5. IEEE, 2016.
- [48] 3GPP. 3GPP ts 36.321 v14.2.0. evolved universal terrestrial radio access(E-UTRA); medium access control(MAC) protocol specification, March 2017.
- [49] Shadi Al-Sarawi, Mohammed Anbar, Kamal Alieyan, and Mahmood Alzubaidi. Internet of things (iot) communication protocols. In *2017 8th International conference on information technology (ICIT)*, pages 685–690. IEEE, 2017.
- [50] Farzad Samie, Lars Bauer, and Jörg Henkel. Iot technologies for embedded computing: A survey. In *Proceedings of the Eleventh IEEE/ACM/IFIP International Conference on Hardware/Software Codesign and System Synthesis*, page 8. ACM, 2016.

- [51] Michele Magno, Christian Spagnol, Luca Benini, and Emanuel Popovici. A low power wireless node for contact and contactless heart monitoring. *Microelectronics Journal*, 45(12):1656–1664, 2014.
- [52] Alberto Ferrari, Pieter Ginis, Michael Hardegger, Filippo Casamassima, Laura Rocchi, and Lorenzo Chiari. A mobile kalman-filter based solution for the real-time estimation of spatio-temporal gait parameters. *IEEE transactions on neural systems and rehabilitation engineering*, 24(7):764–773, 2016.
- [53] Andrea Giovanni Cutti, Alberto Ferrari, Pietro Garofalo, Michele Raggi, Angelo Cappello, and Adriano Ferrari. ‘outwalk’: a protocol for clinical gait analysis based on inertial and magnetic sensors. *Medical & biological engineering & computing*, 48(1):17, 2010.
- [54] Justin J Kavanagh and Hylton B Menz. Accelerometry: a technique for quantifying movement patterns during walking. *Gait & posture*, 28(1):1–15, 2008.
- [55] D. Brunelli, E. Farella, L. Rocchi, M. Dozza, L. Chiari, and L. Benini. Bio-feedback system for rehabilitation based on a wireless body area network. In *Fourth Annual IEEE International Conference on Pervasive Computing and Communications Workshops (PERCOMW’06)*, pages 5 pp.–531. IEEE, 2006.
- [56] Gabriele Bleser, Bertram Taetz, and Paul Lukowicz. Human motion capturing and activity recognition using wearable sensor networks. In *Developing Support Technologies*, pages 191–206. Springer, 2018.
- [57] Thomas Provot, Xavier Chimentin, Emeric Oudin, Fabrice Bolaers, and Sébastien Murer. Validation of a high sampling rate inertial measurement unit for acceleration during running. *Sensors*, 17(9):1958, 2017.
- [58] K Govinda. Body fitness monitoring using iot device. In *Contemporary Applications of Mobile Computing in Healthcare Settings*, pages 154–169. IGI Global, 2018.
- [59] Cheng Xu, Jie He, Xiaotong Zhang, Cui Yao, and Po-Hsuan Tseng. Geometrical kinematic modeling on human motion using method of multi-sensor fusion. *Information Fusion*, 41:243–254, 2018.
- [60] Raffaele Gravina, Parastoo Alinia, Hassan Ghasemzadeh, and Giancarlo Fortino. Multi-sensor fusion in body sensor networks: State-of-the-art and research challenges. *Information Fusion*, 35:68–80, 2017.
- [61] Carmen CY Poon, Benny PL Lo, Mehmet Rasit Yuce, Akram Alomainy, and Yang Hao. Body sensor networks: In the era of big data and beyond. *IEEE reviews in biomedical engineering*, 8:4–16, 2015.
- [62] HM Schepers, Matteo Giuberti, and Giovanni Bellusci. Xsens mvn: Consistent tracking of human motion using inertial sensing. In *Xsens Technologies*, pages 1–8. 2018.

- [63] Halim Tannous, Dan Istrate, Aziz Benlarbi-Delai, Julien Sarrazin, Didier Gamet, Marie Ho Ba Tho, and Tien Dao. A new multi-sensor fusion scheme to improve the accuracy of knee flexion kinematics for functional rehabilitation movements. *Sensors*, 16(11):1914, 2016.
- [64] Alberto Leardini, Giada Lullini, Sandro Giannini, Lisa Berti, Maurizio Ortolani, and Paolo Caravaggi. Validation of the angular measurements of a new inertial-measurement-unit based rehabilitation system: comparison with state-of-the-art gait analysis. *Journal of neuroengineering and rehabilitation*, 11(1):136, 2014.
- [65] Angelo Maria Sabatini. Estimating three-dimensional orientation of human body parts by inertial/magnetic sensing. *Sensors*, 11(2):1489–1525, 2011.
- [66] Anton Kos and Anton Umek. Wearable sensor devices for prevention and rehabilitation in healthcare: Swimming exercise with real-time therapist feedback. *IEEE Internet of Things Journal*, 2018.
- [67] Anton Kos, Veljko Milutinović, and Anton Umek. Challenges in wireless communication for connected sensors and wearable devices used in sport biofeedback applications. *Future generation computer systems*, 92:582–592, 2019.
- [68] Pete B Shull, Wisit Jirattigalachote, Michael A Hunt, Mark R Cutkosky, and Scott L Delp. Quantified self and human movement: a review on the clinical impact of wearable sensing and feedback for gait analysis and intervention. *Gait & posture*, 40(1):11–19, 2014.
- [69] Michele Magno, Michael Pritz, Philipp Mayer, and Luca Benini. Deepemote: Towards multi-layer neural networks in a low power wearable multi-sensors bracelet. In *2017 7th IEEE International Workshop on Advances in Sensors and Interfaces (IWASI)*, pages 32–37. IEEE, 2017.
- [70] Arash Atrsaei, Hassan Salarieh, Aria Alasty, and Mohammad Abediny. Human arm motion tracking by inertial/magnetic sensors using unscented kalman filter and relative motion constraint. *Journal of Intelligent & Robotic Systems*, 90(1-2):161–170, 2018.
- [71] Sungphill Moon, Youngbin Park, Dong Wook Ko, and Il Hong Suh. Multiple kinect sensor fusion for human skeleton tracking using kalman filtering. *International Journal of Advanced Robotic Systems*, 13(2):65, 2016.
- [72] Fred Daum. Nonlinear filters: beyond the kalman filter. *IEEE Aerospace and Electronic Systems Magazine*, 20(8):57–69, 2005.
- [73] Rudolph Van Der Merwe and Eric A Wan. The square-root unscented kalman filter for state and parameter-estimation. In *2001 IEEE international conference on acoustics, speech, and signal processing. Proceedings (Cat. No. 01CH37221)*, volume 6, pages 3461–3464. IEEE, 2001.

- [74] David Maidment. Advanced architectures and technologies for the development of wearable devices, 2014.
- [75] Cortex-m0 technical reference manual.
- [76] Alberto Cavallo, Andrea Cirillo, Pasquale Cirillo, Giuseppe De Maria, Pietro Falco, Ciro Natale, and Salvatore Pirozzi. Experimental comparison of sensor fusion algorithms for attitude estimation. *IFAC Proceedings Volumes*, 47(3):7585–7591, 2014.
- [77] Kinetis, "<https://www.nxp.com/products/processors-and-microcontrollers/arm-based-processors-and-mcus/kinetis-cortex-m-mcus:kinetis>".
- [78] Richard Wallace. Antenna selection guide. *Application Note AN058*, 2009.
- [79] Federico Ferrari, Marco Zimmerling, Luca Mottola, and Lothar Thiele. Low-power wireless bus. In *Proceedings of the 10th ACM Conference on Embedded Network Sensor Systems*, pages 1–14. ACM, 2012.
- [80] Angel Corona Alan Collins, Alin Lazar. "hands-on workshop: Using wireless connectivity stacks and tools to create multi-protocol projects for the internet of things (iot) ftf-sds-f0042", 2014.
- [81] Andrea Giovanni Cutti, Andrea Giovanardi, Laura Rocchi, Angelo Davalli, and Rinaldo Sacchetti. Ambulatory measurement of shoulder and elbow kinematics through inertial and magnetic sensors. *Medical & biological engineering & computing*, 46(2):169–178, 2008.
- [82] VCR Appel, RE Garcia, GR Chiqueti, LM Pedro, DMC Cruz, and GAP Cairin. Novel assessment measures of upper-limb function in pre and poststroke rehabilitation: a pilot study. In *2018 7th IEEE International Conference on Biomedical Robotics and Biomechatronics (Biorob)*, pages 479–483. IEEE, 2018.
- [83] Mi Zhang, Belinda Lange, Chien-Yen Chang, Alexander A Sawchuk, and Albert A Rizzo. Beyond the standard clinical rating scales: fine-grained assessment of post-stroke motor functionality using wearable inertial sensors. In *2012 Annual International Conference of the IEEE Engineering in Medicine and Biology Society*, pages 6111–6115. IEEE, 2012.
- [84] Alisa Aguirre. Evaluating upper-extremity (dys) function using inertial measurement unit technology and its applications to resource-constrained settings.
- [85] AB Ericsson. Cellular networks for massive iot—enabling low power wide area applications. *no. January*, pages 1–13, 2016.
- [86] Michele Magno, Vana Jelcic, Bruno Srbinovski, Vedran Bilas, Emanuel Popovici, and Luca Benini. Design, implementation, and performance evaluation of a flexible low-latency nanowatt wake-up radio receiver. *IEEE Transactions on Industrial Informatics*, 12(2):633–644, 2016.

- [87] Aamir Mahmood, Emiliano Sisinni, Lakshmikanth Guntupalli, Raul Rondon, Syed Ali Hassan, and Mikael Gidlund. Scalability analysis of a lora network under imperfect orthogonality. *IEEE Transactions on Industrial Informatics*, 2018.
- [88] Mauricio de Castro Tomé, Pedro HJ Nardelli, and Hirley Alves. Long-range low-power wireless networks and sampling strategies in electricity metering. *IEEE Transactions on Industrial Electronics*, 66(2):1629–1637, 2019.
- [89] Michele Magno, Tommaso Polonelli, Luca Benini, and Emanuel Popovici. A low cost, highly scalable wireless sensor network solution to achieve smart led light control for green buildings. *IEEE Sensors Journal*, 15(5):2963–2973, 2015.
- [90] Peng Duan, Yunjian Jia, Liang Liang, Jonathan Rodriguez, Kazi Mohammed Saidul Huq, and Guojun Li. Space-reserved cooperative caching in 5g heterogeneous networks for industrial iot. *IEEE Transactions on Industrial Informatics*, 14(6):2715–2724, 2018.
- [91] Carles Gomez, Juan Carlos Veras, Rafael Vidal, Lluís Casals, and Josep Paradells. A sigfox energy consumption model. *Sensors*, 19(3):681, 2019.
- [92] Aloÿs Augustin, Jiazi Yi, Thomas Clausen, and William Mark Townsley. A study of lora: Long range & low power networks for the internet of things. *Sensors*, 16(9):1466, 2016.
- [93] Francesco Orfei, Chiara Benedetta Mezzetti, and Francesco Cottone. Vibrations powered lora sensor: An electromechanical energy harvester working on a real bridge. In *2016 IEEE SENSORS*, pages 1–3. IEEE, 2016.
- [94] Thomas Ameloot, Patrick Van Torre, and Hendrik Rogier. A compact low-power lora iot sensor node with extended dynamic range for channel measurements. *Sensors*, 18(7):2137, 2018.
- [95] Mads Lauridsen, Rasmus Krigslund, Marek Rohr, and Germán Madueno. An empirical nb-iot power consumption model for battery lifetime estimation. In *Ieee Vts... Vehicular Technology Conference*, 2018.
- [96] Liang Zhou, Dan Wu, Jianxin Chen, and Zhenjiang Dong. Greening the smart cities: Energy-efficient massive content delivery via d2d communications. *IEEE Transactions on Industrial Informatics*, 14(4):1626–1634, 2018.
- [97] Olakunle Elijah, Tharek Abdul Rahman, Igbafe Orikumhi, Chee Yen Leow, and MHD Nour Hindia. An overview of internet of things (iot) and data analytics in agriculture: Benefits and challenges. *IEEE Internet of Things Journal*, 5(5):3758–3773, 2018.
- [98] Chun Yeow Yeoh, Abdullah bin Man, Qazi Mamoon Ashraf, and Ahmad Kam-sani Samingan. Experimental assessment of battery lifetime for commercial off-the-shelf nb-iot module. In *2018 20th International Conference on Advanced Communication Technology (ICACT)*, pages 223–228. IEEE, 2018.

- [99] Vitaly Petrov, Andrey Samuylov, Vyacheslav Begishev, Dmitri Moltchanov, Sergey Andreev, Konstantin Samouylov, and Yevgeni Koucheryavy. Vehicle-based relay assistance for opportunistic crowdsensing over narrowband iot (nb-iot). *IEEE Internet of Things journal*, 5(5):3710–3723, 2018.
- [100] Seongjung Ha, Hyoungwon Seo, Youngjunn Moon, Dongjun Lee, and Junho Jeong. A novel solution for nb-iot cell coverage expansion. In *2018 Global Internet of Things Summit (GIoTS)*, pages 1–5. IEEE, 2018.
- [101] LoRa SX1276. 868/915mhz rf transceiver module, 2019.
- [102] N2XXX series Sara. Ublox sara n211 nb-iot module for europe; cat nb1, 2019.
- [103] Tian Wang, Md Zakirul Alam Bhuiyan, Guojun Wang, Md Arafatur Rahman, Jie Wu, and Jiannong Cao. Big data reduction for a smart city’s critical infrastructural health monitoring. *IEEE Communications Magazine*, 56(3):128–133, 2018.
- [104] Floris Van den Abeele, Jetmir Haxhibeqiri, Ingrid Moerman, and Jeroen Hoebeke. Scalability analysis of large-scale lorawan networks in ns-3. *IEEE Internet of Things Journal*, 4(6):2186–2198, 2017.
- [105] Tommaso Polonelli, Davide Brunelli, and Luca Benini. Slotted aloha overlay on lorawan-a distributed synchronization approach. In *2018 IEEE 16th International Conference on Embedded and Ubiquitous Computing (EUC)*, pages 129–132. IEEE, 2018.
- [106] Jetmir Haxhibeqiri, Abdulkadir Karaagac, Floris Van den Abeele, Wout Joseph, Ingrid Moerman, and Jeroen Hoebeke. Lora indoor coverage and performance in an industrial environment: Case study. In *2017 22nd IEEE International Conference on Emerging Technologies and Factory Automation (ETFA)*, pages 1–8. IEEE, 2017.
- [107] LoRa SX1276. 77/78/79 datasheet, rev. 4, 2015.
- [108] Lte e-utra physical layer procedures, ts 36.213 v13.8.0, 2018.
- [109] Maher El Assi, Alia Ghaddar, Samar Tawbi, and Ghaddar Fadi. Resource-efficient floating-point data compression using mas in wsn. *International Journal of Ad Hoc, Sensor & Ubiquitous Computing*, 4(5):13, 2013.
- [110] Toni Adame, Albert Bel, Anna Carreras, Joan Melià-Seguí, Miquel Oliver, and Rafael Pous. Cuidats: An rfid–wsn hybrid monitoring system for smart health care environments. *Future Generation Computer Systems*, 78:602–615, 2018.
- [111] Anawarali Suthar, Ravi Patel, and Pratik Patel. Design, development and realization of flexible programmable low-cost wireless sensor nodes for industrial application using iot. 2019.

- [112] 3gpp. "3rd generation partnership project; technical specification group service and system aspects; 3gpp system architecture evolution (sae); security architecture (rel 12) 3gpp ts 33.401 v12.5.0,". Sep. 2012.